# WIMPs or else?
## Using Machine Learning for Dark Matter Detection


Charanjit Khosa
University of Sussex

UNIVERSITY
OF SUSSEX


**NExT Meeting, University of Sussex, 20th November 2019**

Based on: 1. CKK, Veronica Sanz, Michael Soughton, arXiv: 1910.06058 [hep-ph]
2. CKK, Lucy Mars, Joel Richards, Veronica Sanz [in prep.]

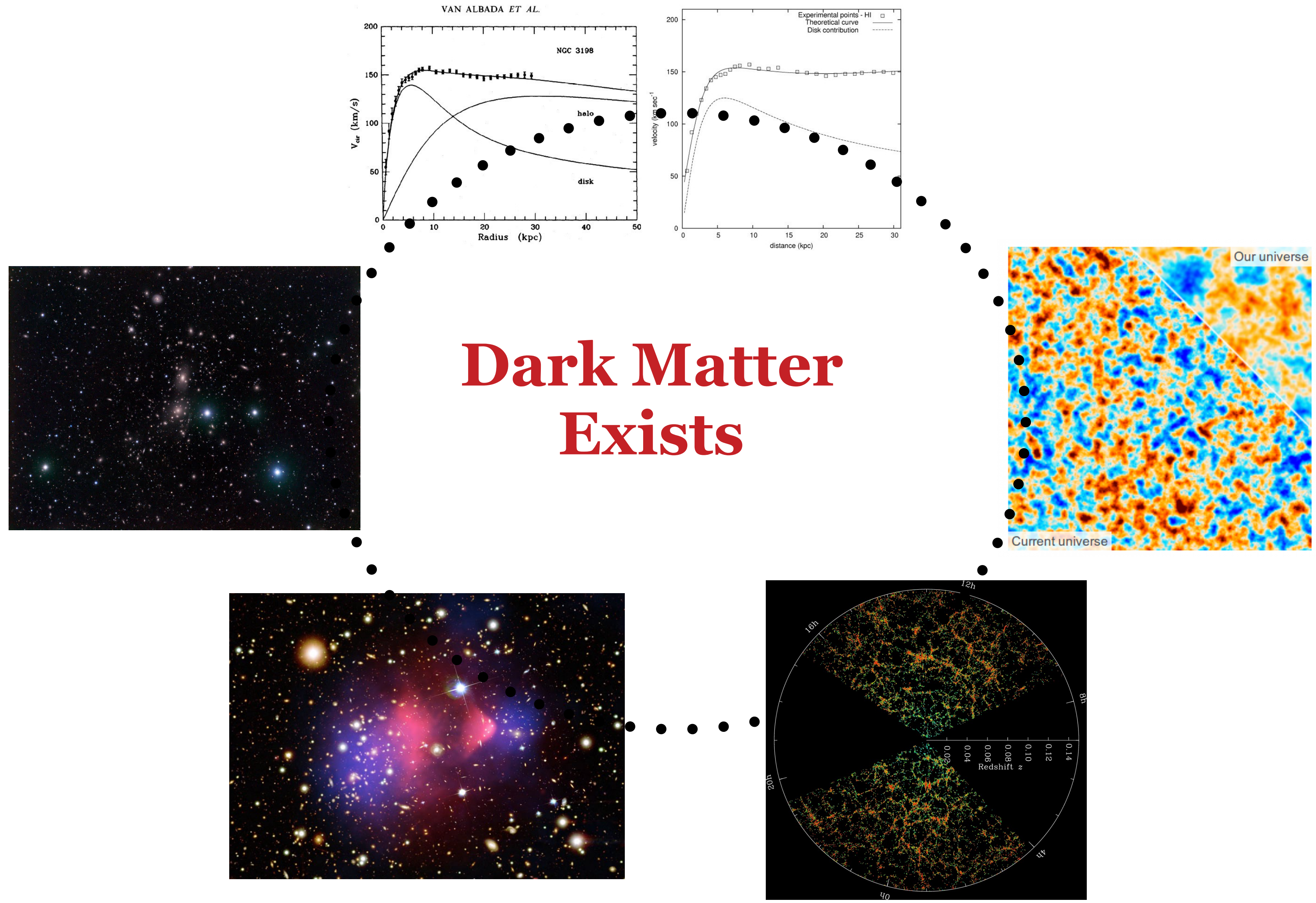

VAN ALBADA ET AL.
NGC 3198
halo
disk
Radius (kpc)
Experimental points - HI
Theoretical curve
Disk contribution
distance (kpc)
Dark Matter
Exists
Our universe
Current universe
Redshift z


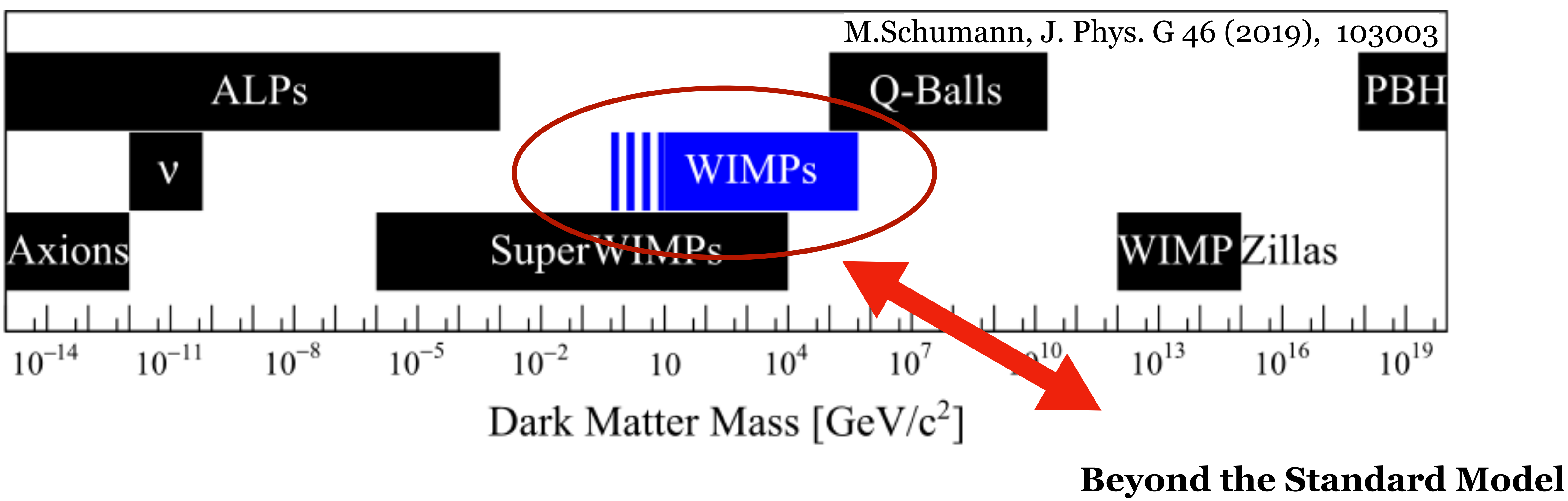

M.Schumann, J. Phys. G 46 (2019), 103003
ALPs
Q-Balls
PBH
ν
WIMPs
Axions
SuperWIMPs
WIMPZillas
$10^{-14}$ $10^{-11}$ $10^{-8}$ $10^{-5}$ $10^{-2}$ 10 $10^{4}$ $10^{7}$ $10^{10}$ $10^{13}$ $10^{16}$ $10^{19}$
Dark Matter Mass [GeV/c$^2$]
Beyond the Standard Model

# Dark Matter Detection: Current Constraints

**MET+X (jet, photon, W/Z (jets/ll),H(b/tau)+HF (b/t) pair+single top)**

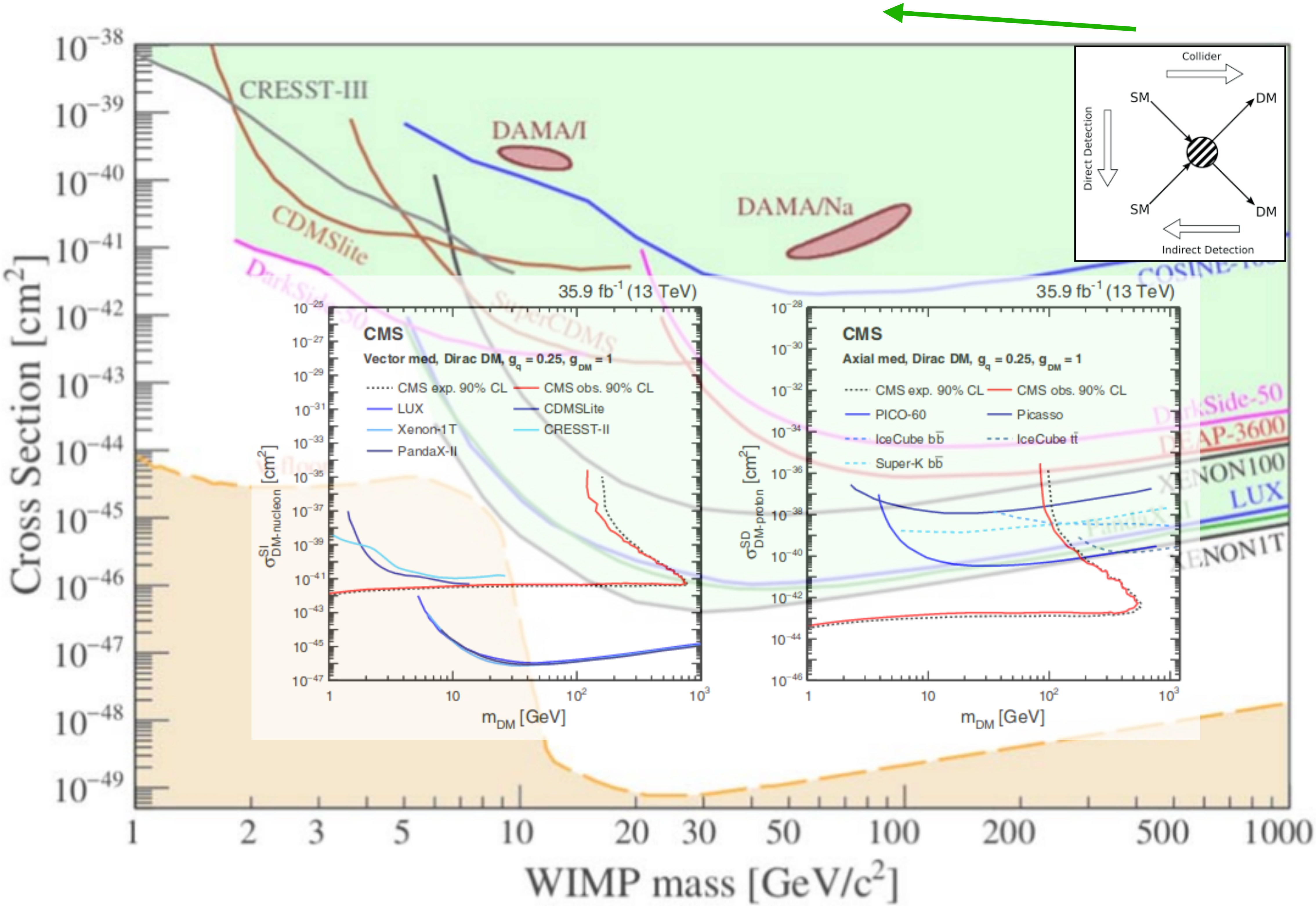


CMS Collaboration, Phys. Rev. D 97 (2018), 092005 M.Schumann, J. Phys. G 46 (2019), 103003

# REVIEW

https://doi.org/10.1038/s41586-018-0361-2

# Machine learning at the energy and intensity frontiers of particle physics

Alexander Radovic[1]*, Mike Williams[2]*, David Rousseau[3], Michael Kagan[4], Daniele Bonacorsi[5,6], Alexander Himmel[7], Adam Aurisano[8], Kazuhiro Terao[4] & Taritree Wongjirad[9]

**Our knowledge of the fundamental particles of nature and their interactions is summarized by the standard model of particle physics. Advancing our understanding in this field has required experiments that operate at ever higher energies and intensities, which produce extremely large and information-rich data samples. The use of machine-learning techniques is revolutionizing how we interpret these data samples, greatly increasing the discovery potential of present and future experiments. Here we summarize the challenges and opportunities that come with the use of machine learning at the frontiers of particle physics.**

**Table 1 | Effect of machine learning on the discovery and study of the Higgs boson**

| Analysis | Years of data collection | Sensitivity without machine learning | Sensitivity with machine learning | Ratio of $P$ values | Additional data required |
|---|---|---|---|---|---|
| CMS[24] $H \to \gamma\gamma$ | 2011–2012 | $2.2\sigma$, $P = 0.014$ | $2.7\sigma$, $P = 0.0035$ | 4.0 | 51% |
| ATLAS[43] $H \to \tau^+\tau^-$ | 2011–2012 | $2.5\sigma$, $P = 0.0062$ | $3.4\sigma$, $P = 0.00034$ | 18 | 85% |
| ATLAS[99] $VH \to bb$ | 2011–2012 | $1.9\sigma$, $P = 0.029$ | $2.5\sigma$, $P = 0.0062$ | 4.7 | 73% |
| ATLAS[41] $VH \to bb$ | 2015–2016 | $2.8\sigma$, $P = 0.0026$ | $3.0\sigma$, $P = 0.00135$ | 1.9 | 15% |
| CMS[100] $VH \to bb$ | 2011–2012 | $1.4\sigma$, $P = 0.081$ | $2.1\sigma$, $P = 0.018$ | 4.5 | 125% |

A. Radovic et al., Nature 560(2018) no. 7716,41

REVIEW

https://doi.org/10.1038/s41586-018-0361-2

# Machine learning at the energy and intensity frontiers of particle physics

Alexander Radovic[1]*, Mike Williams[2]*, David Rousseau[3], Michael Kagan[4], Daniele Bonacorsi[5,6], Alexander Himmel[7], Adam Aurisano[8], Kazuhiro Terao[4] & Taritree Wongjirad[9]

Our knowledge of the fundamental particles of nature and their interactions is summarized by the standard model of particle physics. Advancing our understanding in this field has required experiments that operate at ever higher energies and intensities, which produce extremely large and information-rich data samples. The use of machine-learning techniques is revolutionizing how we interpret these data samples, greatly increasing the discovery potential of present and future experiments. Here we summarize the challenges and opportunities that come with the use of machine learning at the frontiers of particle physics.

## Machine Learning techniques increase the discovery potential of the experiments

**Table 1 | Effect of machine learning on the discovery and study of the Higgs boson**

| Analysis | Years of data collection | Sensitivity without machine learning | Sensitivity with machine learning | Ratio of $P$ values | Additional data required |
|---|---|---|---|---|---|
| CMS[24] $H\to\gamma\gamma$ | 2011–2012 | $2.2\sigma$, $P=0.014$ | $2.7\sigma$, $P=0.0035$ | 4.0 | 51% |
| ATLAS[43] $H\to\tau^+\tau^-$ | 2011–2012 | $2.5\sigma$, $P=0.0062$ | $3.4\sigma$, $P=0.00034$ | 18 | 85% |
| ATLAS[99] $VH\to bb$ | 2011–2012 | $1.9\sigma$, $P=0.029$ | $2.5\sigma$, $P=0.0062$ | 4.7 | 73% |
| ATLAS[41] $VH\to bb$ | 2015–2016 | $2.8\sigma$, $P=0.0026$ | $3.0\sigma$, $P=0.00135$ | 1.9 | 15% |
| CMS[100] $VH\to bb$ | 2011–2012 | $1.4\sigma$, $P=0.081$ | $2.1\sigma$, $P=0.018$ | 4.5 | 125% |

A. Radovic et al., Nature 560(2018) no. 7716,41

nature COMMUNICATIONS

ARTICLE

Received 19 Feb 2014 | Accepted 4 Jun 2014 | Published 2 Jul 2014 DOI: 10.1038/ncomms5308

# Searching for exotic particles in high-energy physics with deep learning

P. Baldi[1], P. Sadowski[1] & D. Whiteson[2]

Collisions at high-energy particle colliders are a traditionally fruitful source of exotic particle discoveries. Finding these rare particles requires solving difficult signal-versus-background classification problems, hence machine-learning approaches are often used. Standard approaches have relied on 'shallow' machine-learning models that have a limited capacity to learn complex nonlinear functions of the inputs, and rely on a painstaking search through manually constructed nonlinear features. Progress on this problem has slowed, as a variety of techniques have shown equivalent performance. Recent advances in the field of deep learning make it possible to learn more complex functions and better discriminate between signal and background classes. Here, using benchmark data sets, we show that deep-learning methods need no manually constructed inputs and yet improve the classification metric by as much as 8% over the best current approaches. This demonstrates that deep-learning approaches can improve the power of collider searches for exotic particles.

Signal

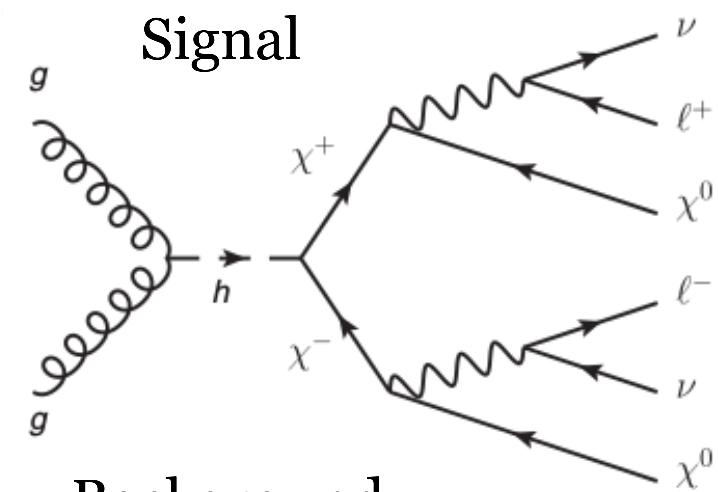


Background

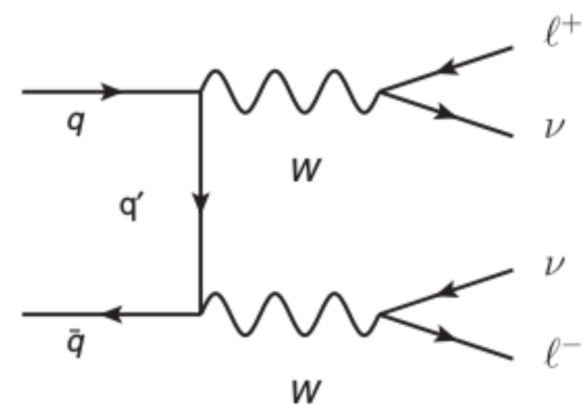


## SUSY benchmark:

**chargino production (lepton+MET final state)**

| Technique | Low-level | High-level | Complete |
|---|---|---|---|
| *AUC* | | | |
| BDT | 0.850 (0.003) | 0.835 (0.003) | 0.863 (0.003) |
| NN | 0.867 (0.002) | 0.863 (0.001) | 0.875 (<0.001) |
| NN$_{dropout}$ | 0.856 (<0.001) | 0.859 (<0.001) | 0.873 (<0.001) |
| DN | 0.872 (0.001) | 0.865 (0.001) | 0.876 (<0.001) |
| DN$_{dropout}$ | 0.876 (<0.001) | 0.869 (<0.001) | 0.879 (<0.001) |
| *Discovery significance* | | | |
| NN | $6.5\sigma$ | $6.2\sigma$ | $6.9\sigma$ |
| DN | $7.5\sigma$ | $7.3\sigma$ | $7.6\sigma$ |

BDT, boosted decision tree; DN, deep neural network; NN, shallow neural network; SUSY, supersymmetry particle.

**Low-level features:** $p_T^{l_1}, p_T^{l_2}, \sum p_T^j, MET, N_j$

**High-level features:** **Axial MET**, $M_{T_2}$, **razor quantities**

# Deep Learning methods improve the reach of the collider searches for new physics searches

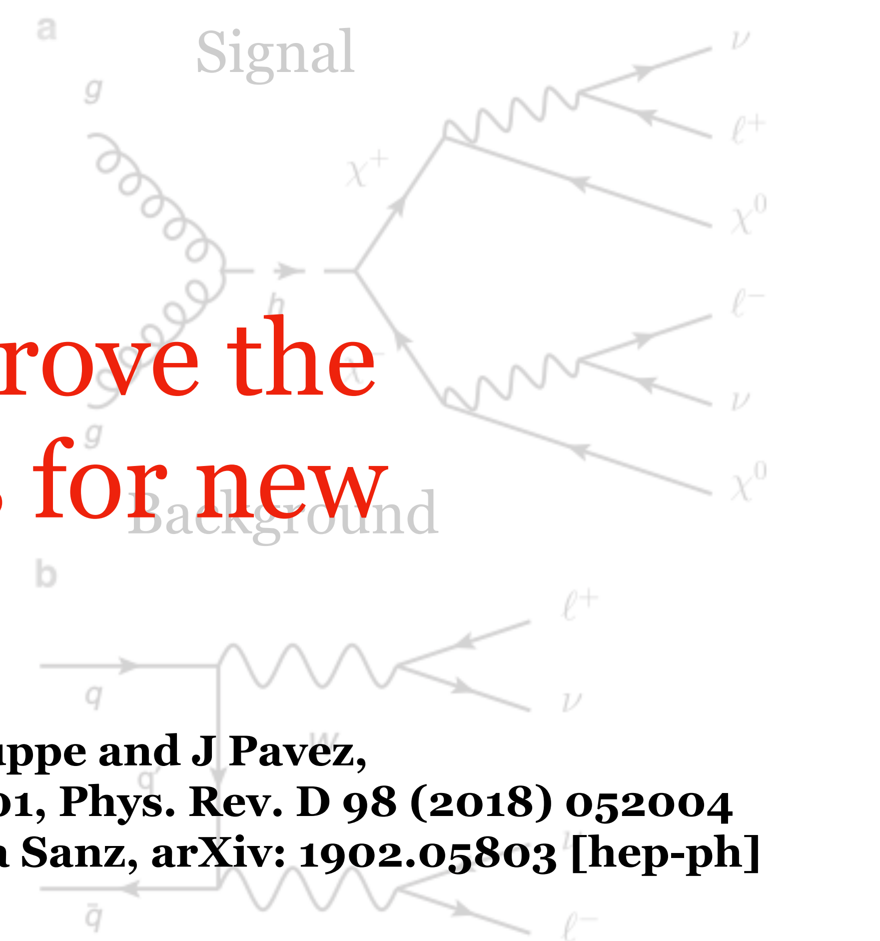


- **SMEFT (new physics deformations)** — J. Brehmer, K. Cranmer, G. Louppe and J Pavez, Phys. Rev. Lett. 121 (2018) 111801, Phys. Rev. D 98 (2018) 052004; Felipe F. Freitas, CKK, Veronica Sanz, arXiv: 1902.05803 [hep-ph]
- **Top tagging** — G.Kasieczka, T.Plehn, M.Russell and T.Schell, JHEP 1705 (2017) 006
- **Novelty detection** — J. Hajer, Y.Y. Li, T. Liu and H. Wang, arXiv: 1807.10261[hep-ph]
- **Anomaly detection** — M. Farina, Y. Nakai and D. Shih, arXiv: 1808.08992[hep-ph]
- **Cosmological phase transitions** — M.L.Piscopo, M.Spannowsky and P.Waite, arXiv:1902.05563 [hep-ph]
- **DijetGAN** — R.Di Sipio, M.Faucci Giannelli et al, arXiv:1903.02433 [hep-ex]
- **many more..**

# DM at LHC: Monojet Channel

| Model | Mass | Type of coupling |
|---|---|---|
| SUSY1 | $m_{\tilde{\chi}^0} = 100$ GeV | Bino-like |
| SUSY2 | $m_{\tilde{\chi}^0} = 200$ GeV | Bino-like |
| SUSY3 | $m_{\tilde{\chi}^0} = 300$ GeV | Bino-like |
| ALP | negligible | gluon-ALP |
| EFT | negligible | 4-fermion |

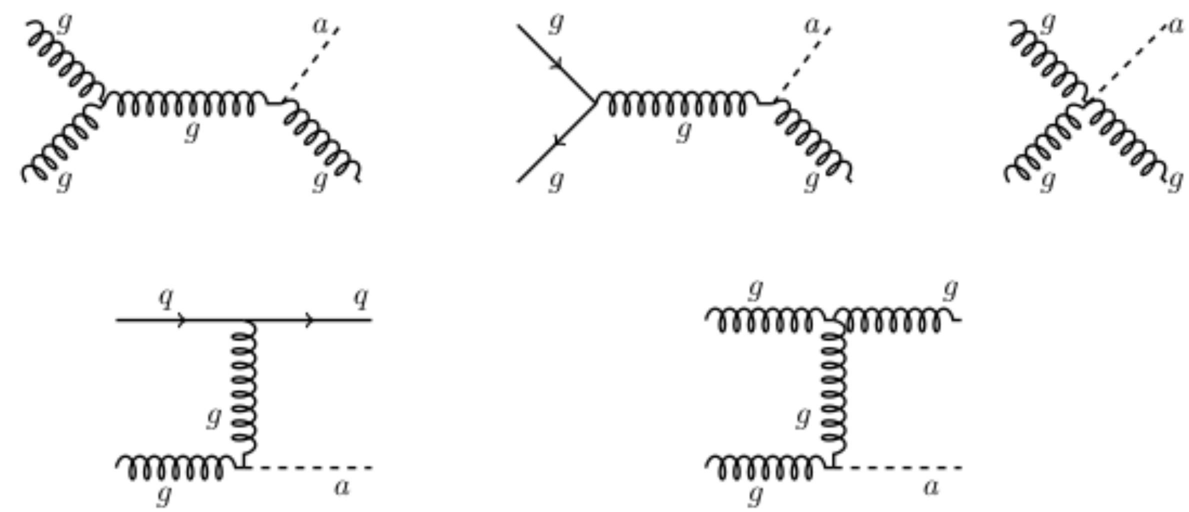

($a$) Monojet process in linear ALPs

**Axion-Like particles (ALPs) could decay after being produced but not inside the detector**

$$\mathscr{L}_a \supset -\frac{g_{agg}}{2} a\, \mathbf{Tr}\left[G_{\mu\nu}\tilde{G}^{\mu\nu}\right]$$

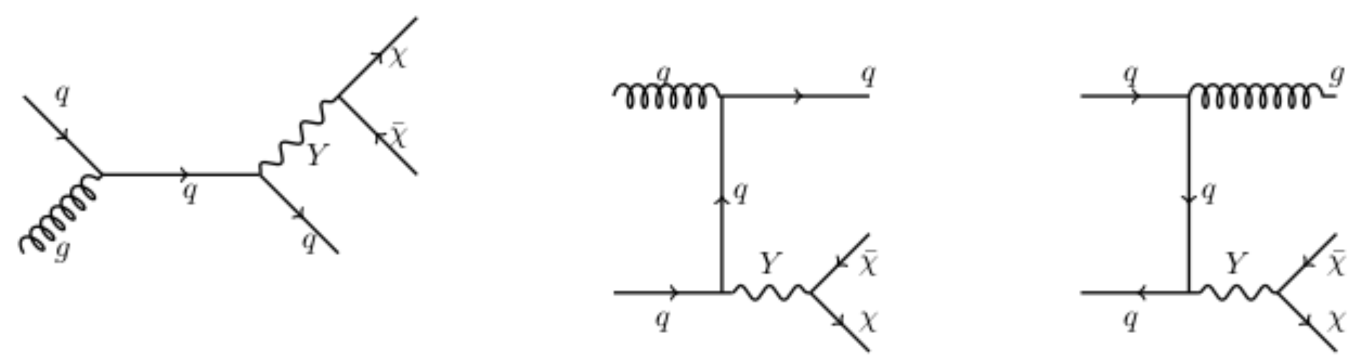

($b$) Monojet process in case of spin 1 mediator

**Simplified models: spin-1 mediator**

$$\mathscr{L}_Y = \bar{\chi}\gamma_\mu g_\chi^V \chi Y^\mu$$

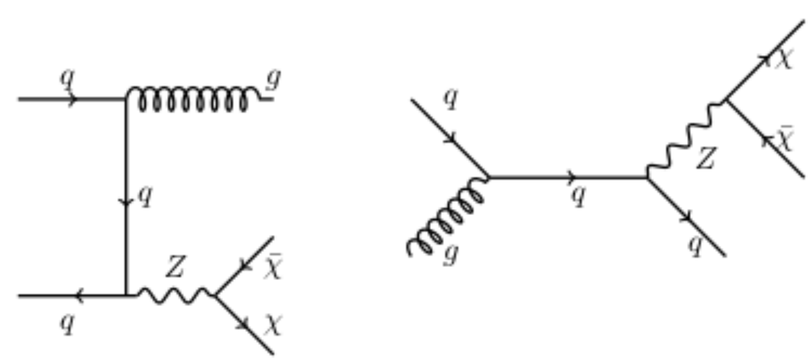

($c$) Monojet process in MSSM

CKK, Veronica Sanz, Michael Soughton, arXiv: 1910.06058 [hep-ph]

# Analysis set-up

**LO, parton level analysis**

$p_T^j(MET), \eta^j, \phi^j$ $\quad$ $p_T^j > 130\text{GeV}$

$\sqrt{s} =$ 14 TeV, 400K events
using MC@NLO Madgraph

SUSY-WIMP $\quad$ $pp \to \tilde{\chi}_1^0 \tilde{\chi}_1^0 j$

ALPs $\quad$ $pp \to aj$

EFT, spin-1 mediator $\quad$ $pp \to \chi\bar{\chi}j$

Feynrules Model :
MSSM-SLHA2,ALPsEFT, DMSimp

**NLO, detector level analysis**

200K events
DELPHES (ATLAS default run card)

$p_T^{j_1}, p_T^{j_2}, \eta^{j_1}, \eta^{j_2}, \text{MET}, \Delta\phi_{j_1 j_2}, \Delta\phi_{MET}^{j_1}, \Delta\phi_{MET}^{j_2}$ $\quad$ $p_T^{j_1} > 130\text{GeV}, p_T^{j_2} > 25\text{GeV}$

CKK, Veronica Sanz, Michael Soughton, arXiv: 1910.06058 [hep-ph]

# Kinematic Distributions

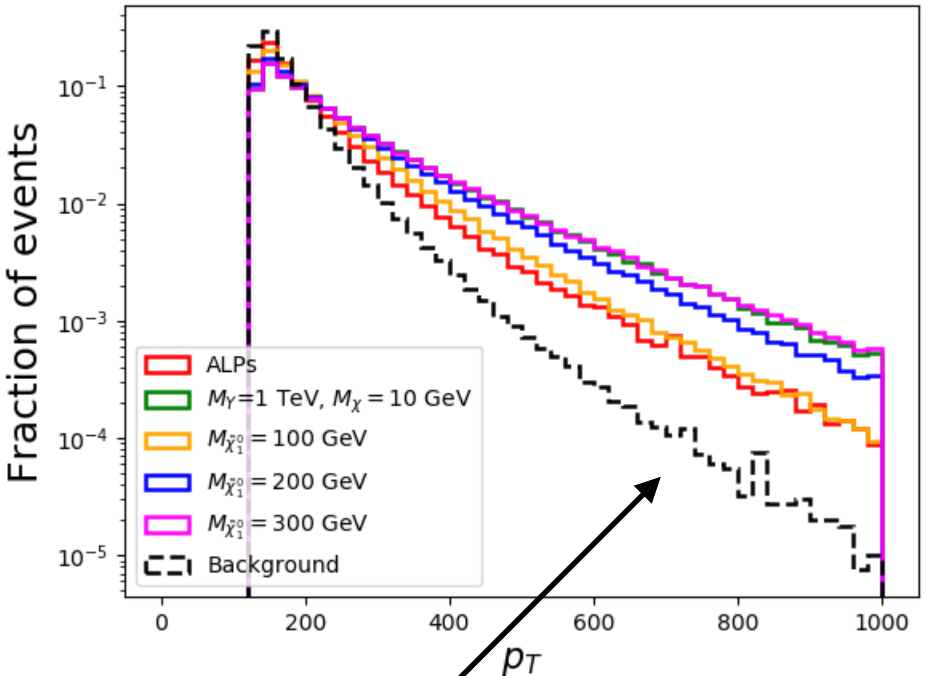


**Transverse momentum of the jet**

$pp \to Z(\to \nu\bar{\nu})j$

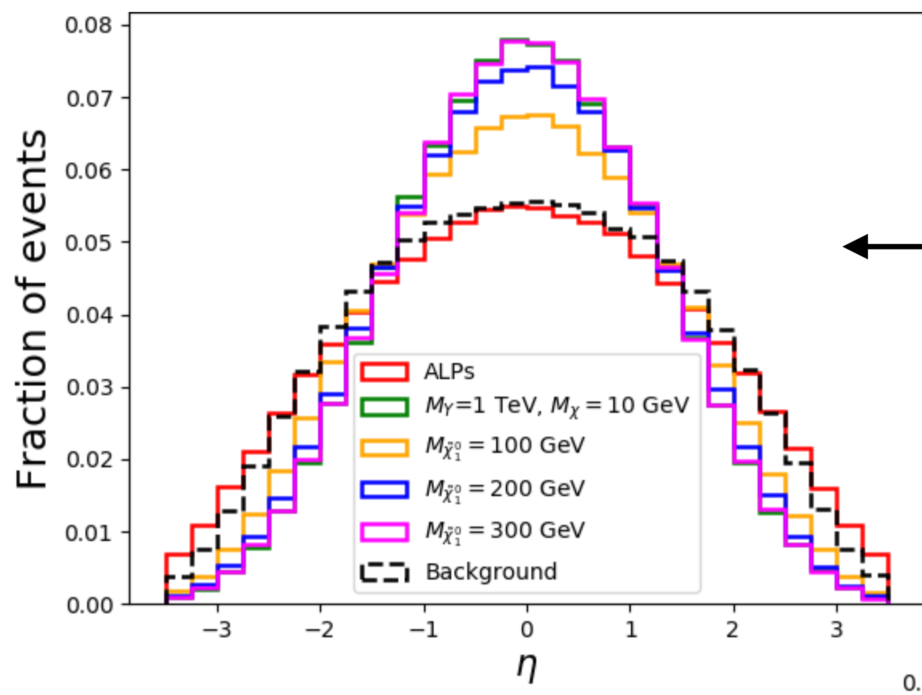


**ALP has similar distribution as SM background**

**Azimuthal angular distribution,**
**No preferred direction for the WIMP**

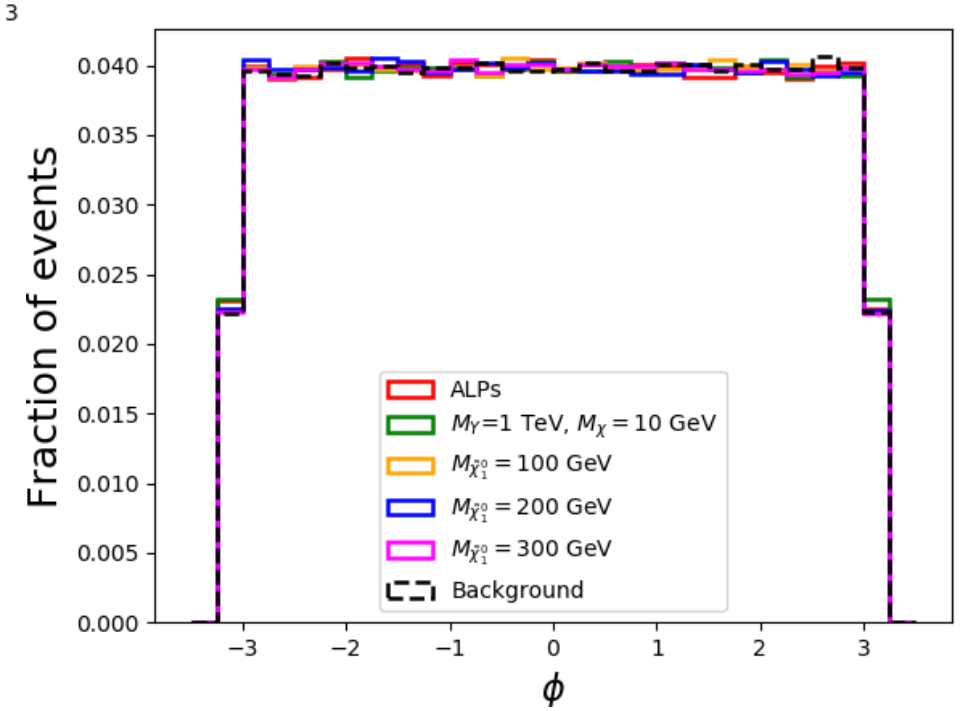

# (Deep) Neural Network

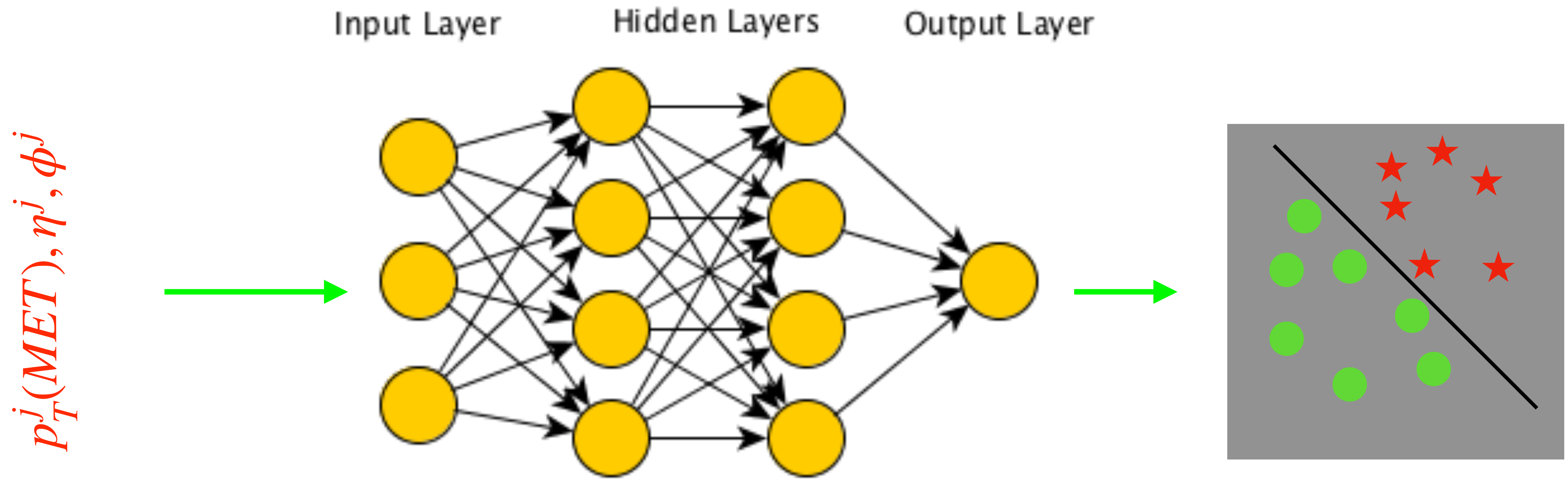


- **Training set: Test set = 70 %: 30% (data scaling)**
- **Hidden layers: 5 (optimised)**
- **Activation function: ReLu**
- **Dropouts: 0.2**
- **Loss function: Binary Cross-entropy**

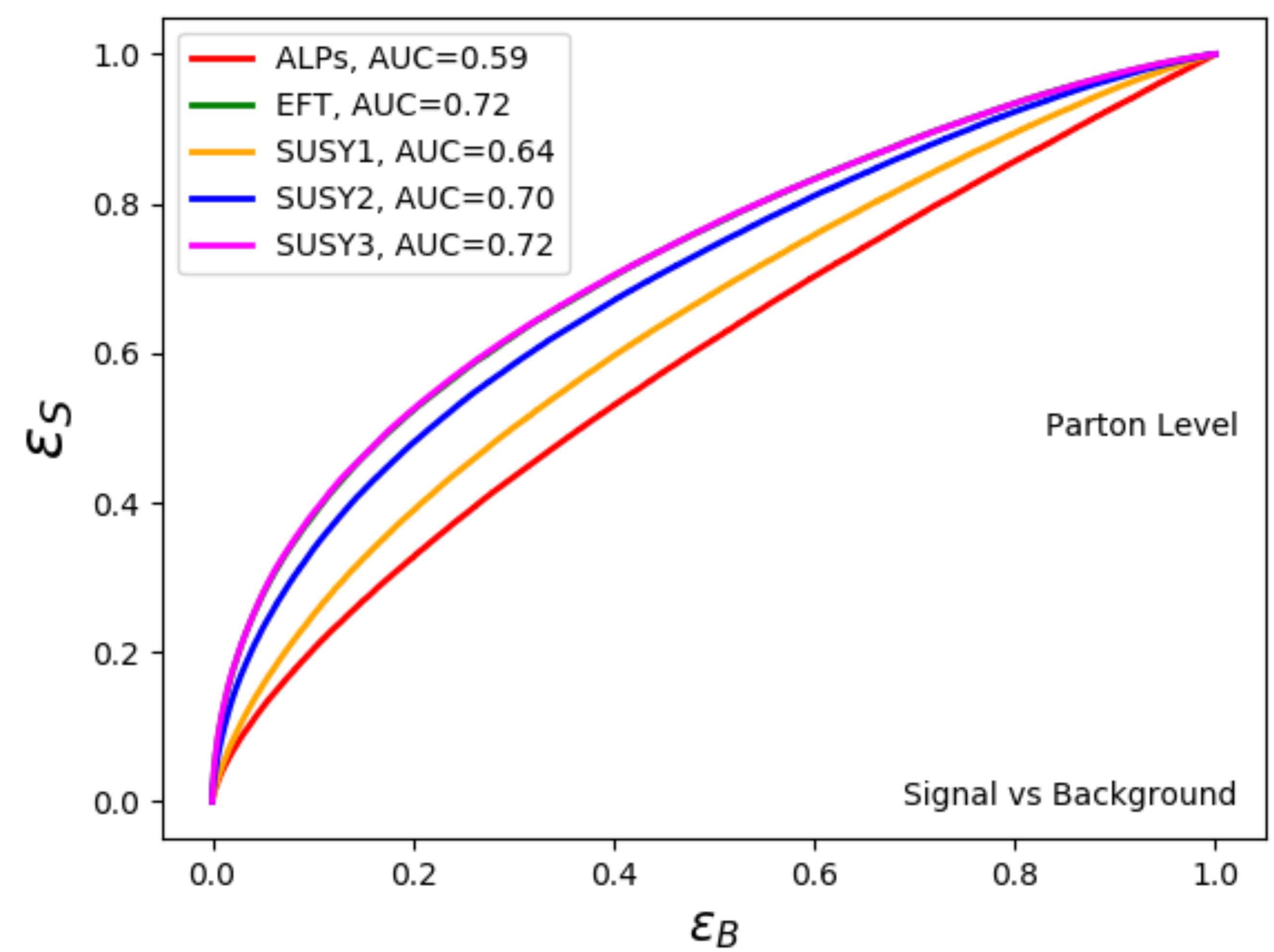


$\epsilon_S$ : **Signal Selection**
$\epsilon_B$ : $1-$**Background Rejection**
**AUC: Area under the ROC curve**

# DM Characterization

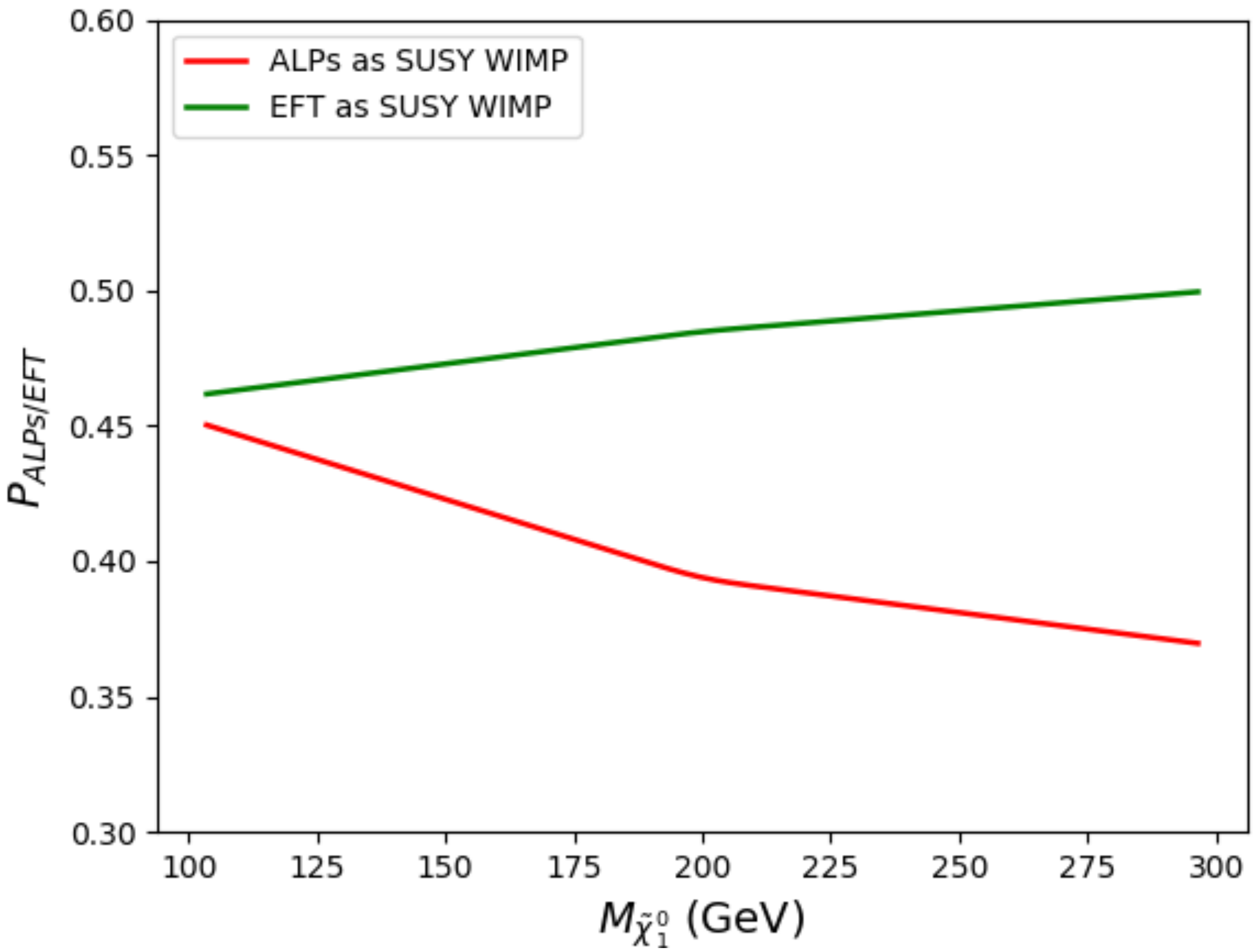


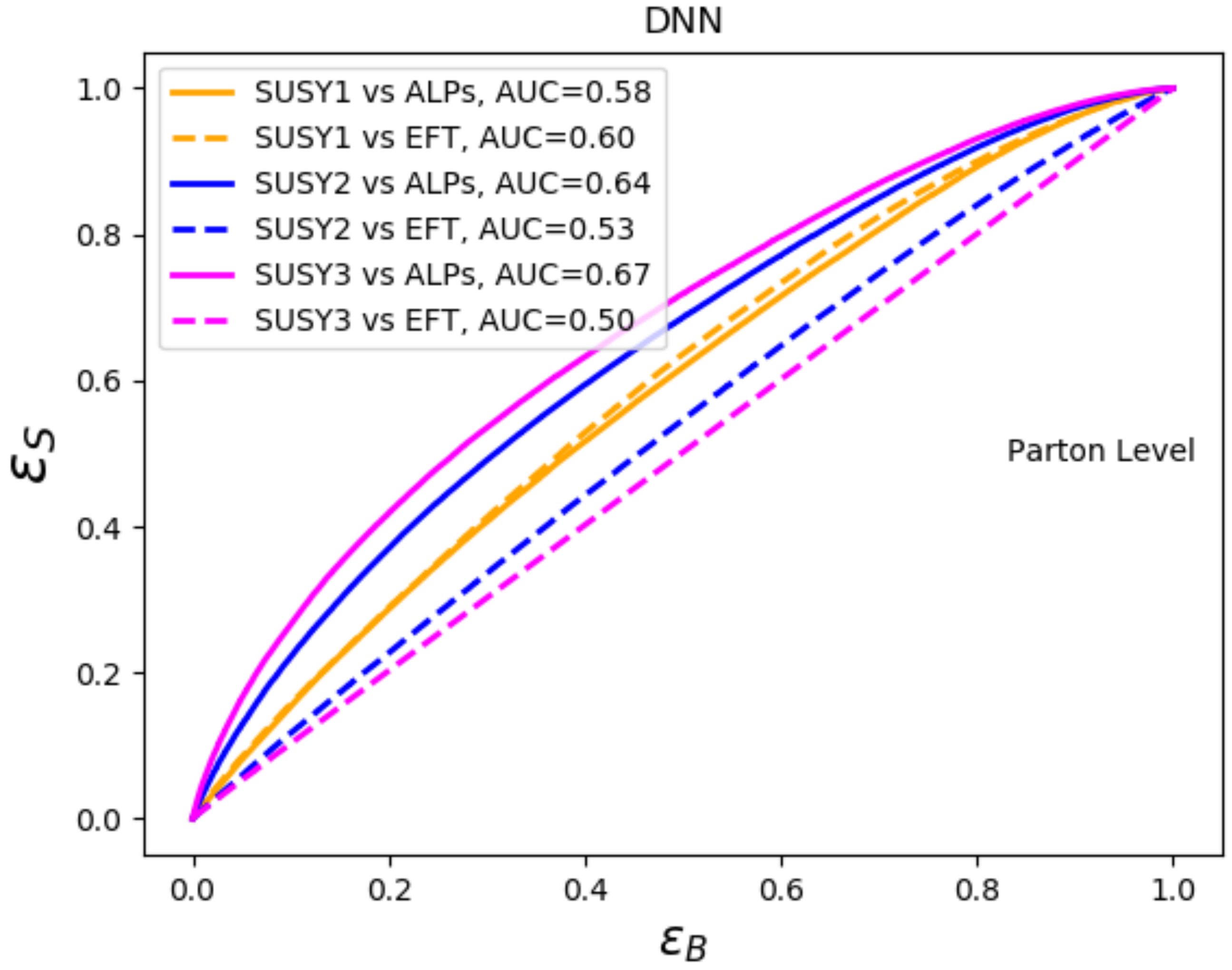

# 2D Distributions (LO Parton Level)

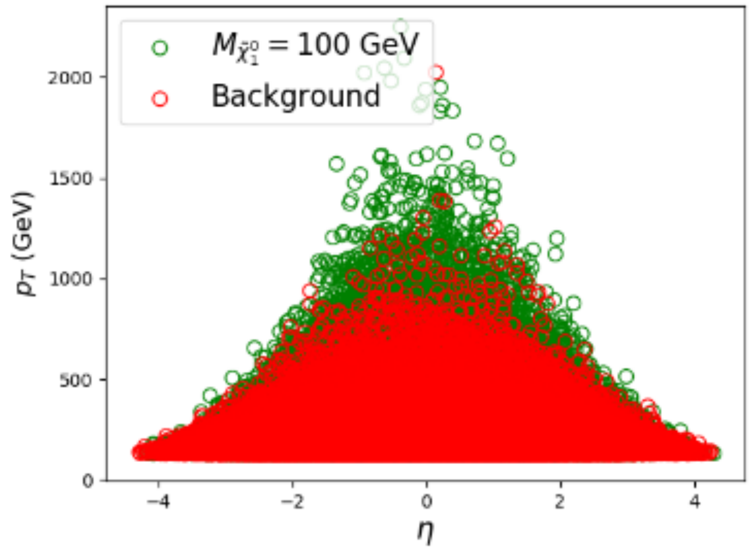


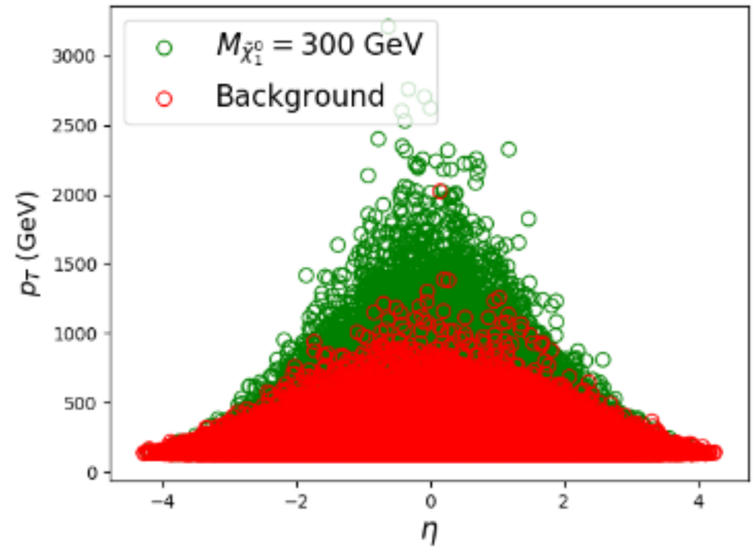


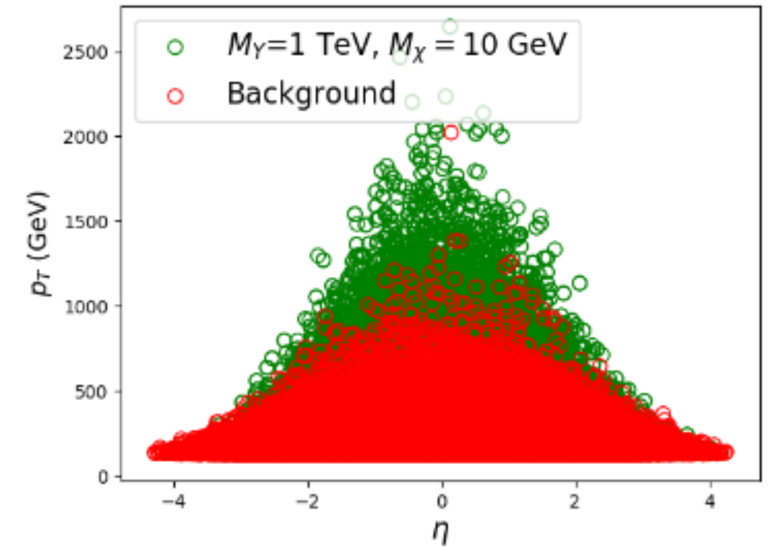


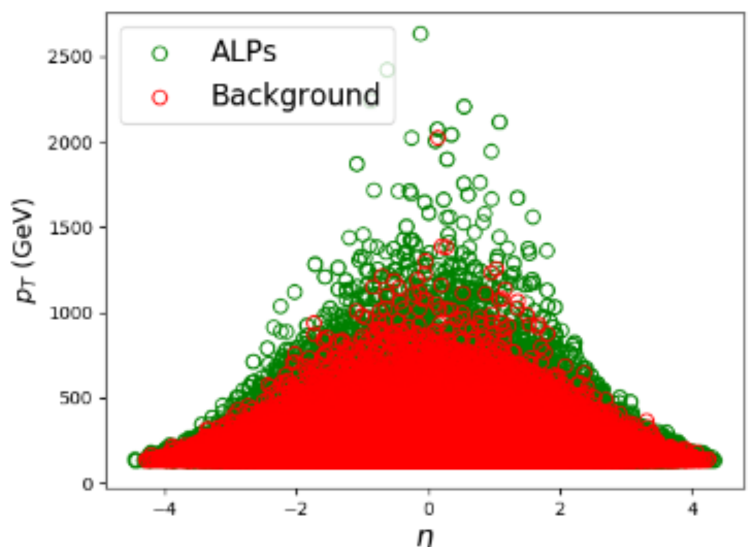


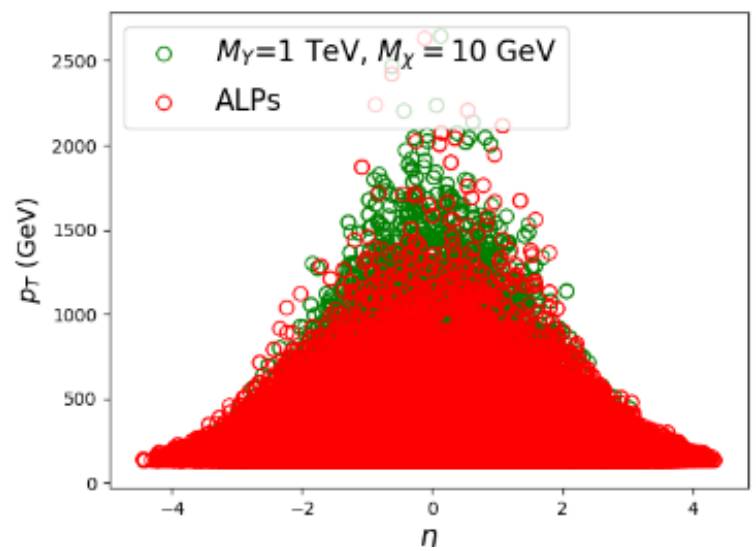


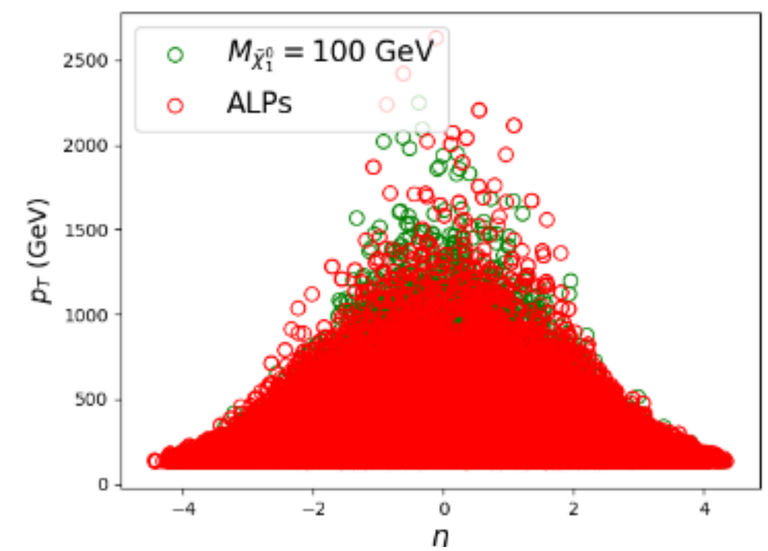


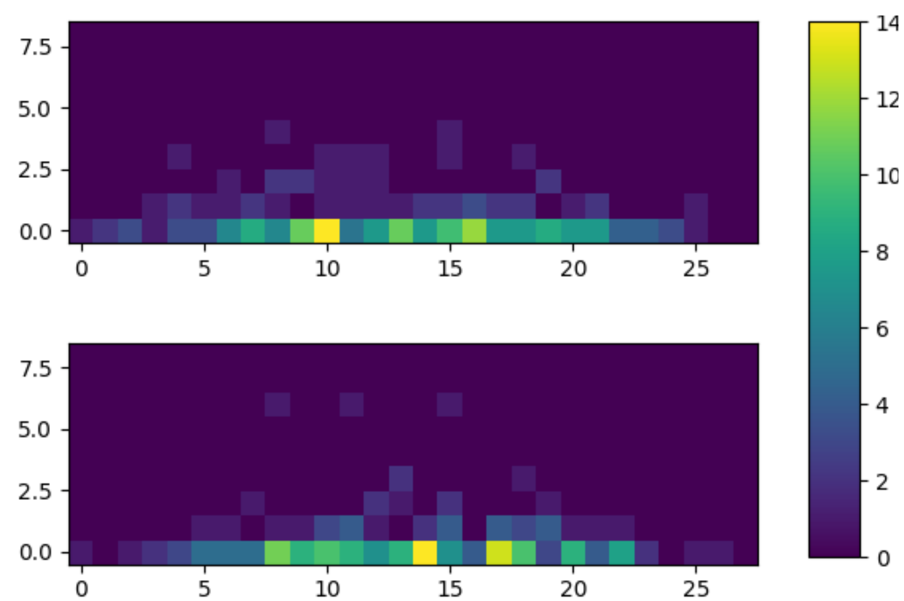

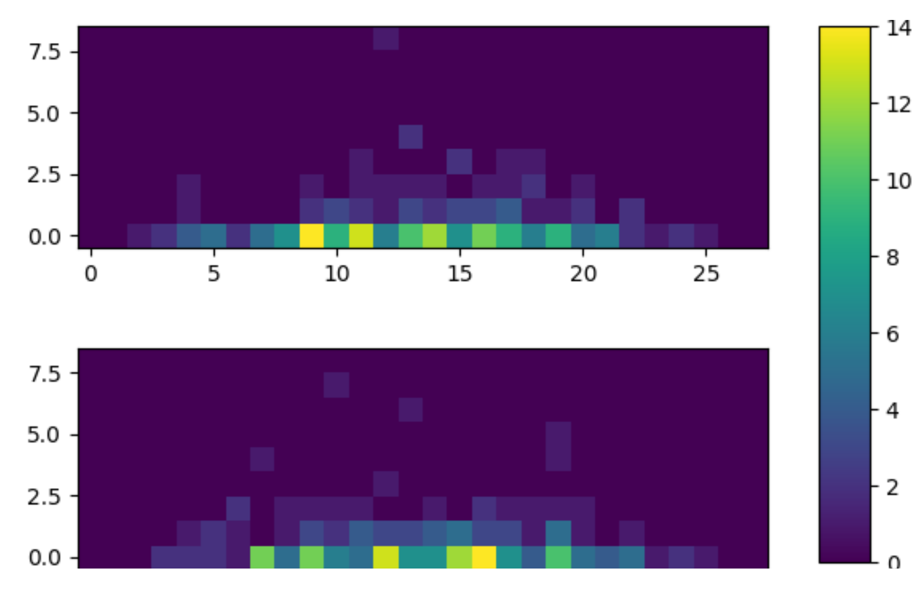

# DNN for 2D Histograms

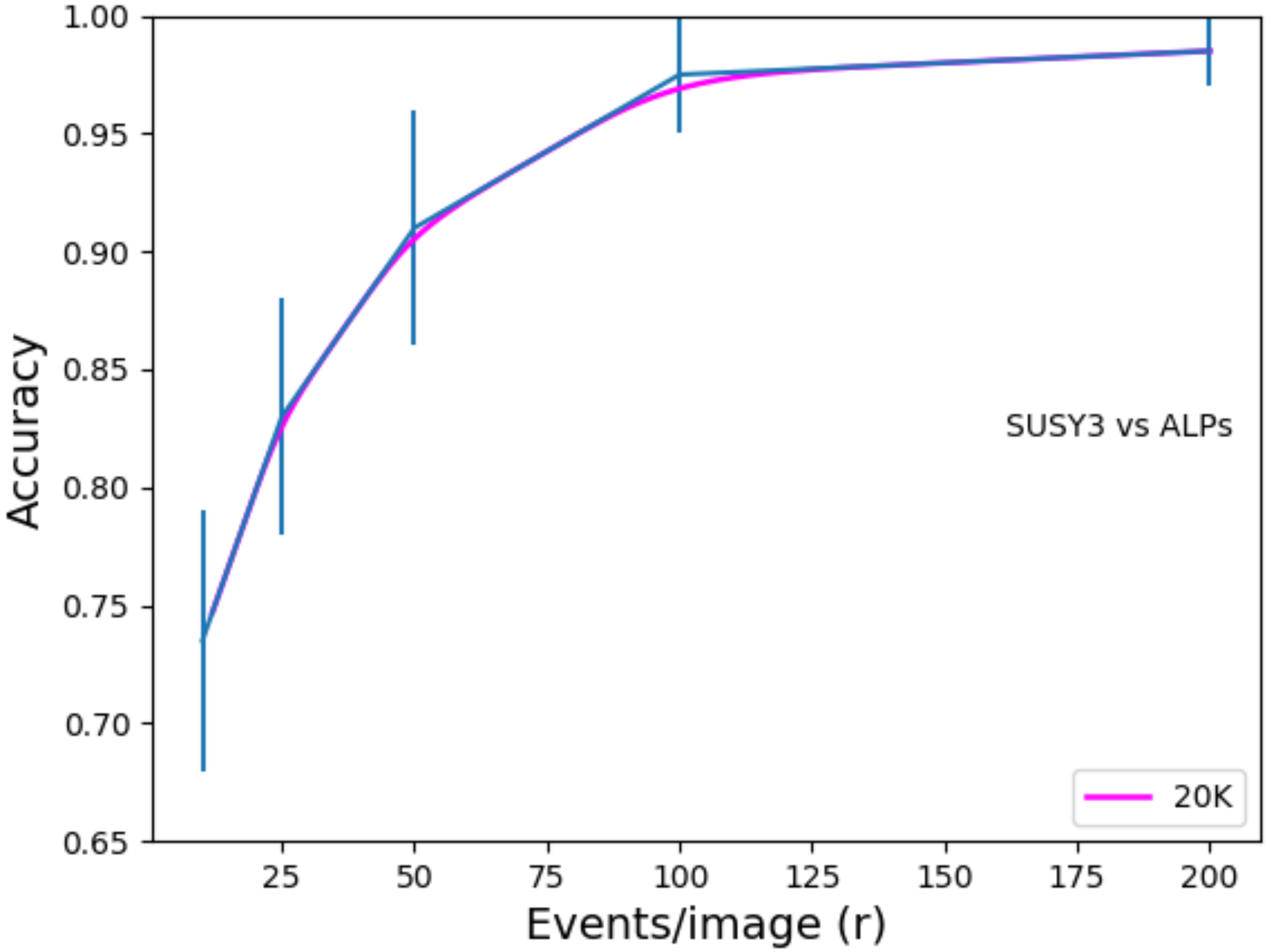


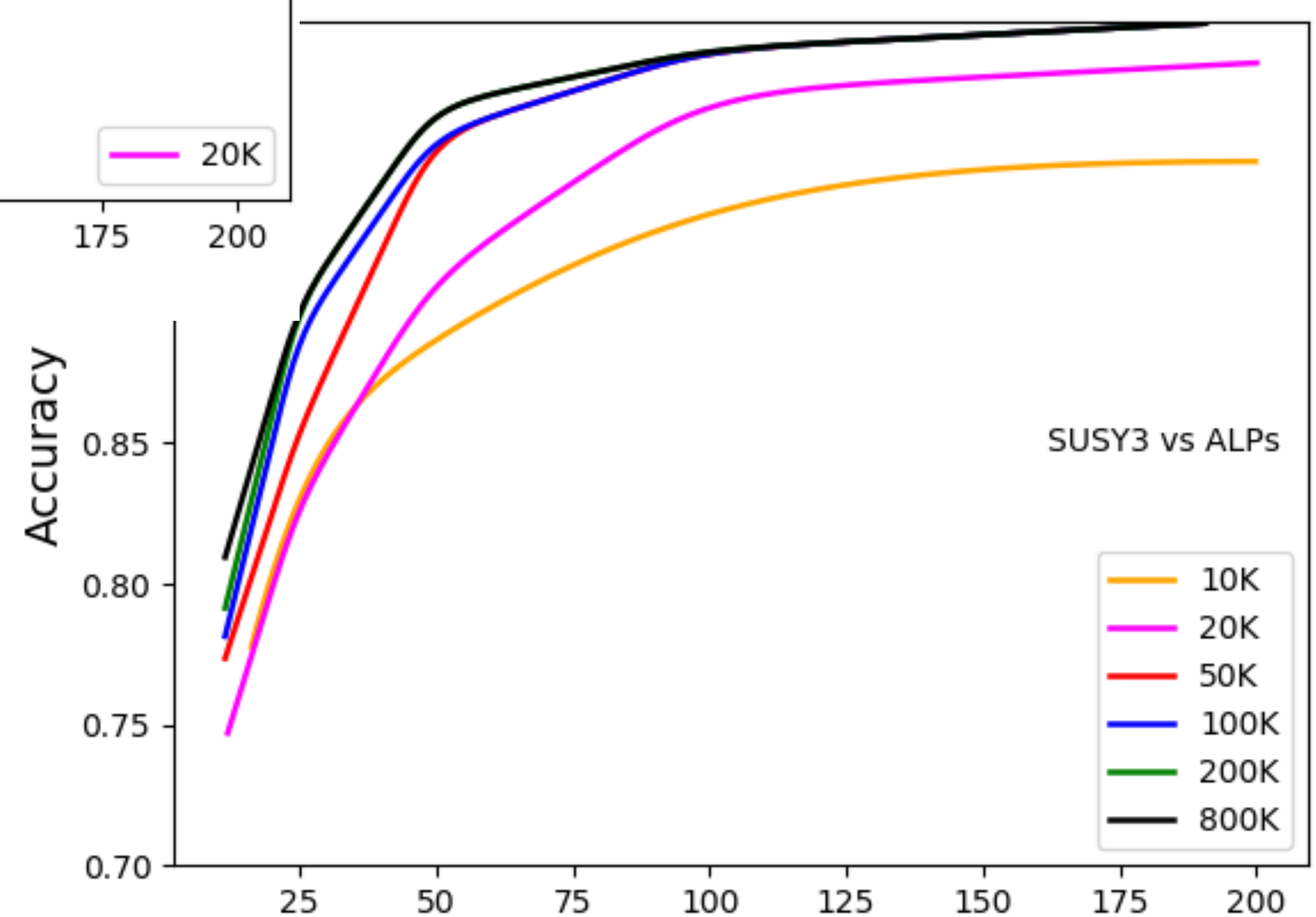

# Dijet Case

**Same NN Architecture**

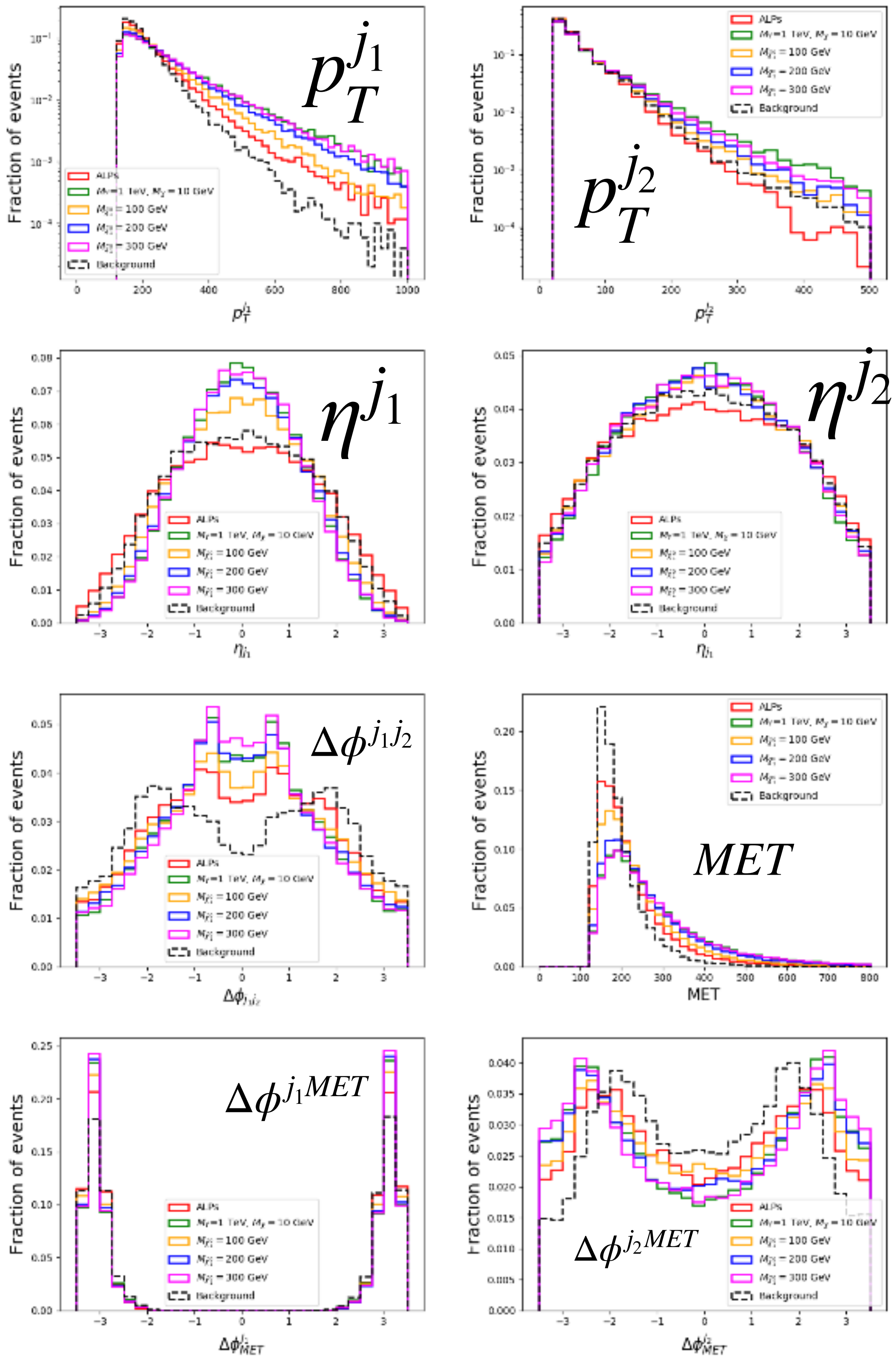


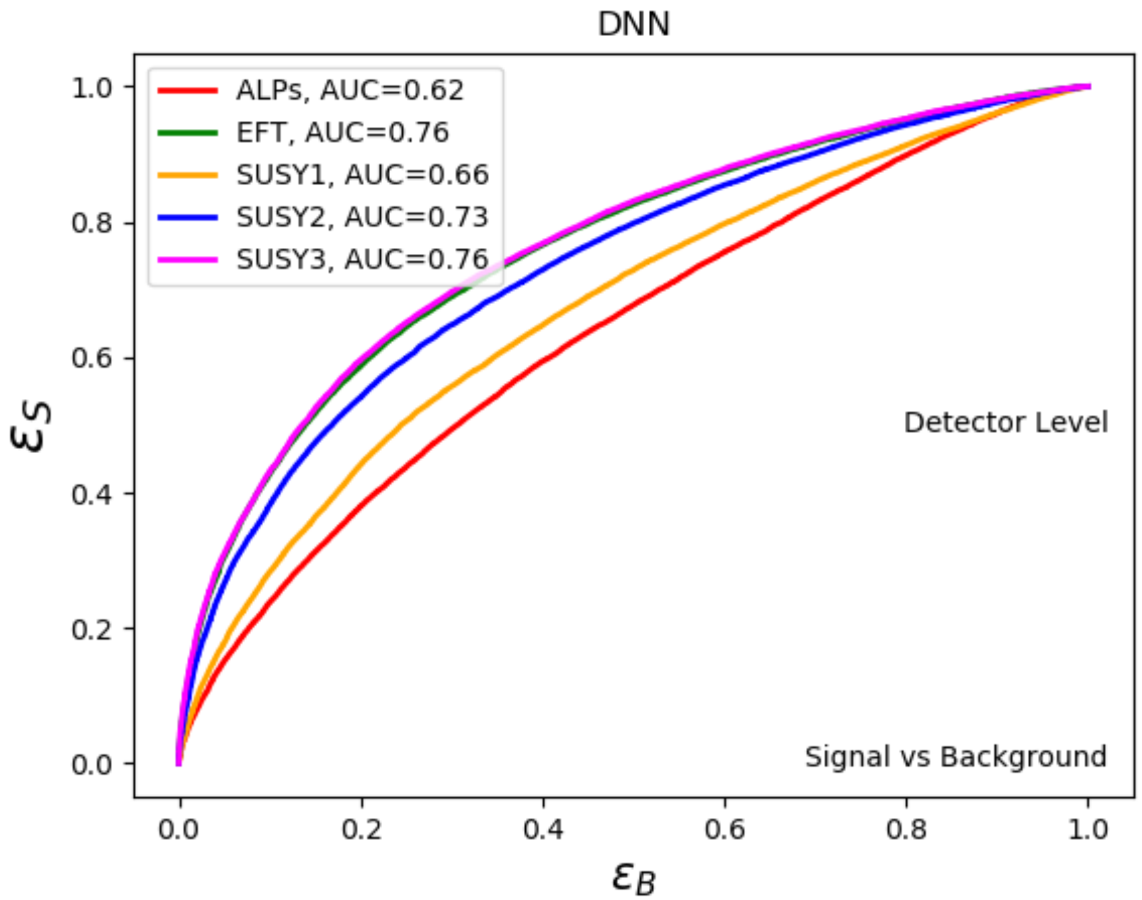

# TPC for Xenon1T Experiment

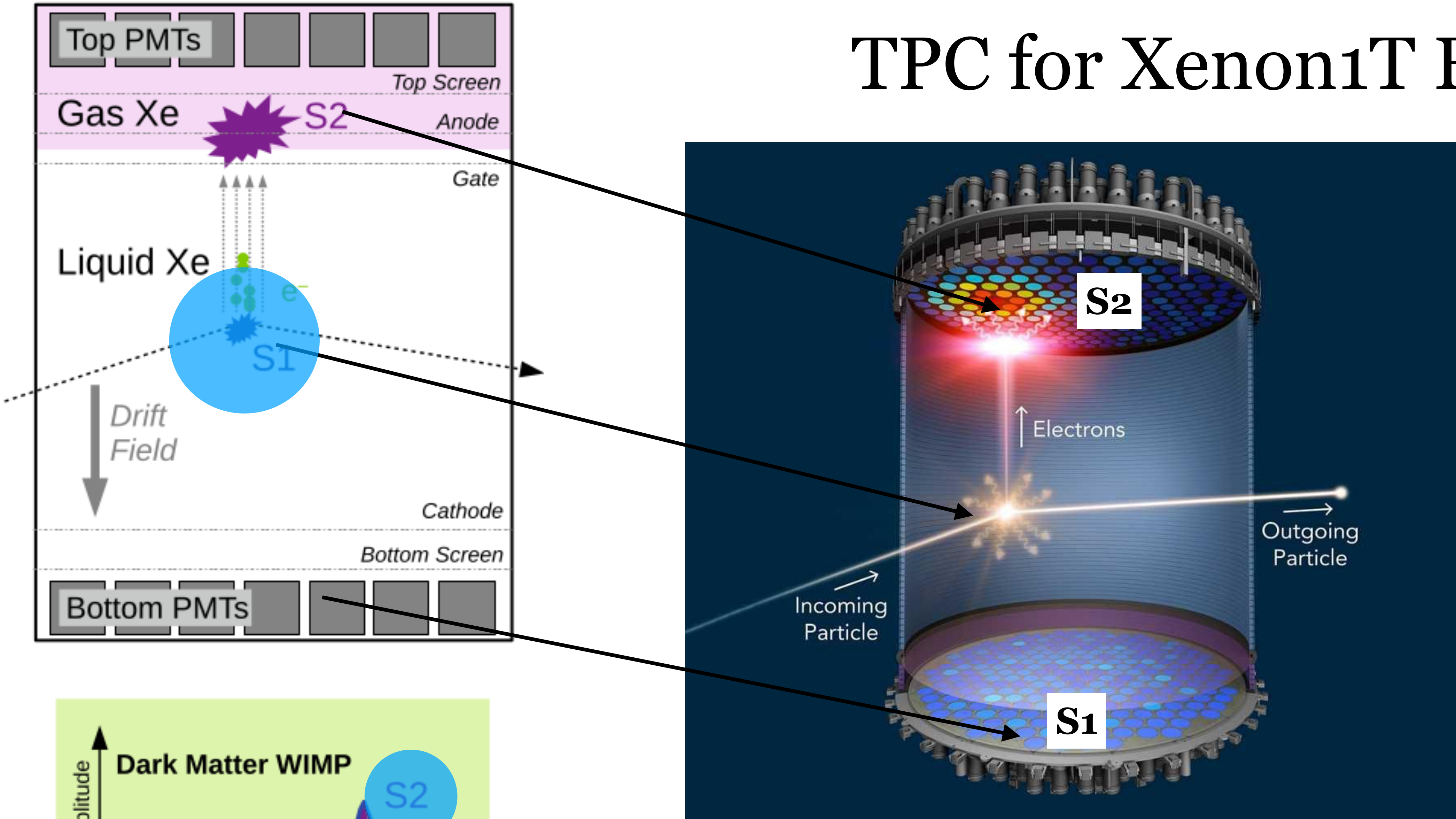


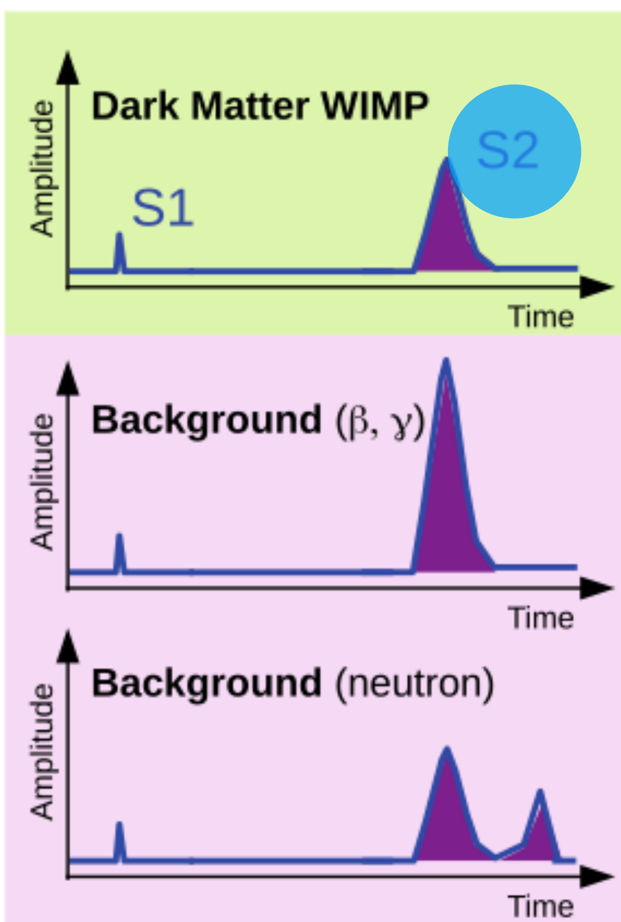


Eur. Phys. J. C (2017) 77:881

**Dual-Phase TPC:**

- **Particle interacts with LXe**
- **Prompt scintillation, S1**
- **Ionisation electrons drift upwards due to $E_{drift}$**
- **Extracted using $E_{extraction}$ at GXe**
- **Delayed signal, S2**

# TPC output as images

| Name | Expected number of events |
|---|---|
| Electronic recoils (ER) | 61.879487 |
| CNNS ($\nu$) | 0.000901 |
| Radiogenic neutrons | 0.058570 |
| Accidental coincidences (acc) | 0.220000 |
| Wall leakage (wall) | 0.520000 |
| Anomalous (anom) | 0.090004 |
| 500 GeV/$c^2$, $10^{-45}$ cm$^2$ WIMP | 35.029005 |

TABLE I. Expected number of events for each type of background within the fiducial mass and a 500 GeV/$c^2$, $10^{-45}$ cm$^2$ WIMP (Generated using Laidbax).

## Simulation Tools for XENON1T

**Laidbax**
**Wimprates**
**Blueice**
→ **FAX** → **PAX**

**WIMP event**

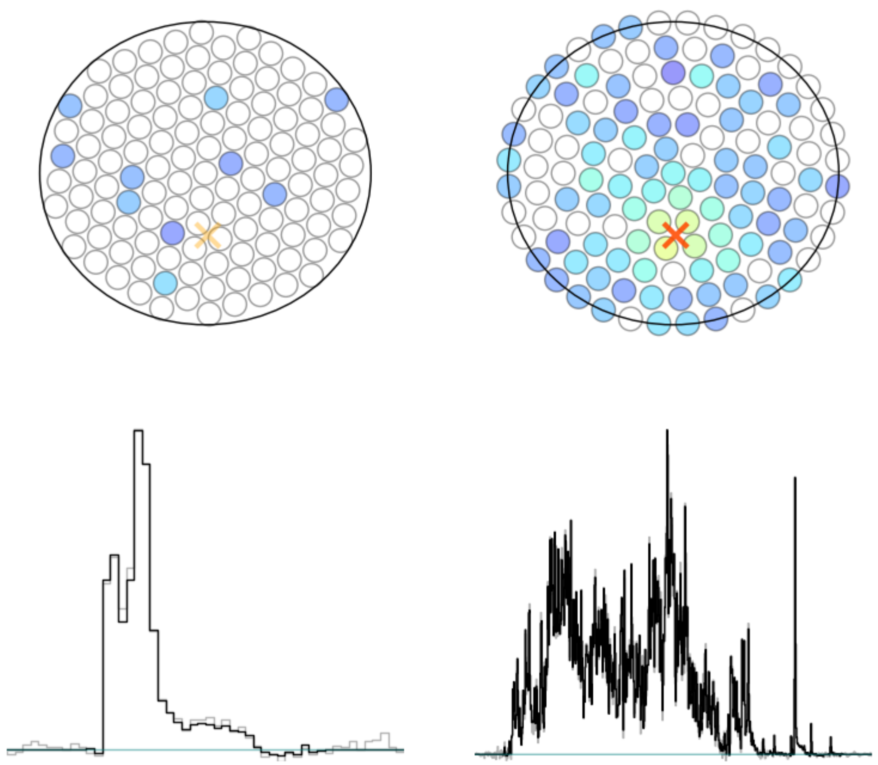

**ER background**

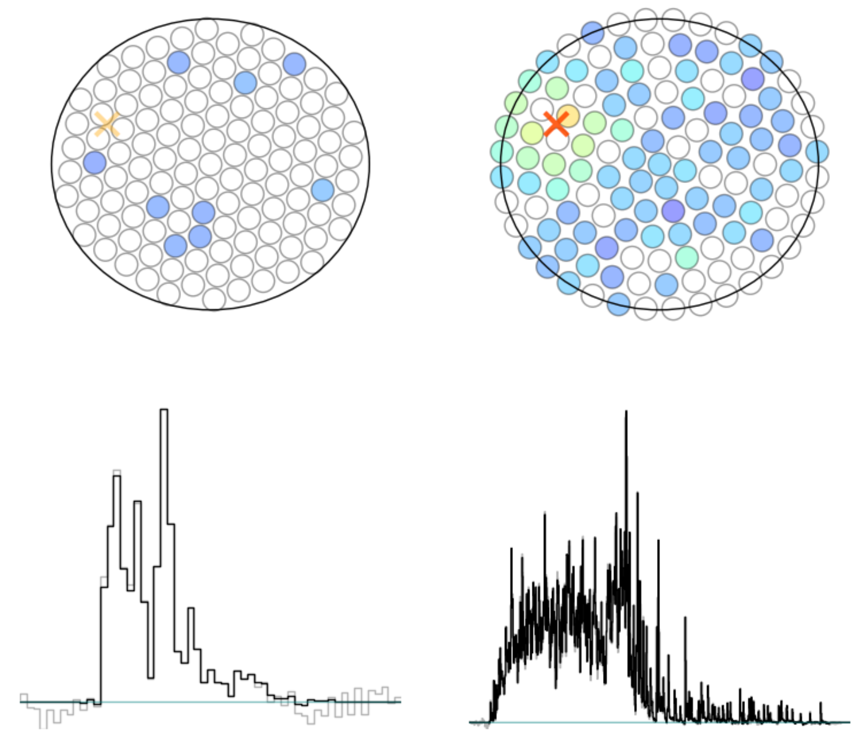

**https://github.com/XENON1T/pax**
**https://github.com/XENON1T/laidbax**
**Aalbers, J. (2018) *Dark Matter Search with XENON1T* (Doctoral dissertation, University of Amsterdam)**

# Convolutional Neural  Network

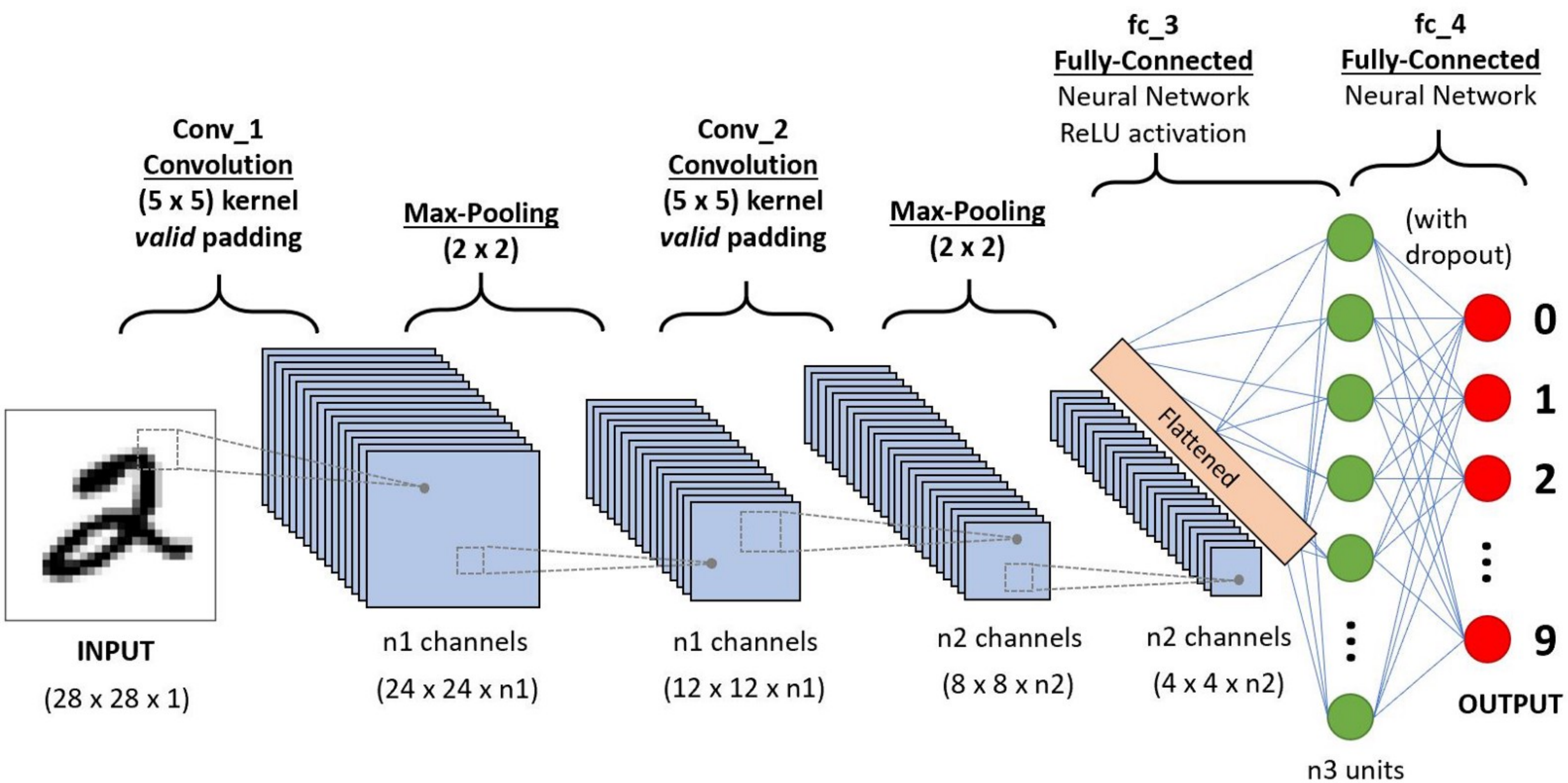


- **Convolutional layer: detect edges**
- **Pooling: compress the information**
- **Classification: (fully) connected hidden layers**

# WIMP versus ER background

- **CNN:**
  - **2 Convolution layers + ReLU activation function**
  - **20 Neurons per layer**
  - **Pooling layer:**
    - **Max Pooling**
    - **Flatten**
    - **ReLU activation function**
  - **Output layer:**
    - **Sigmoid activation function**

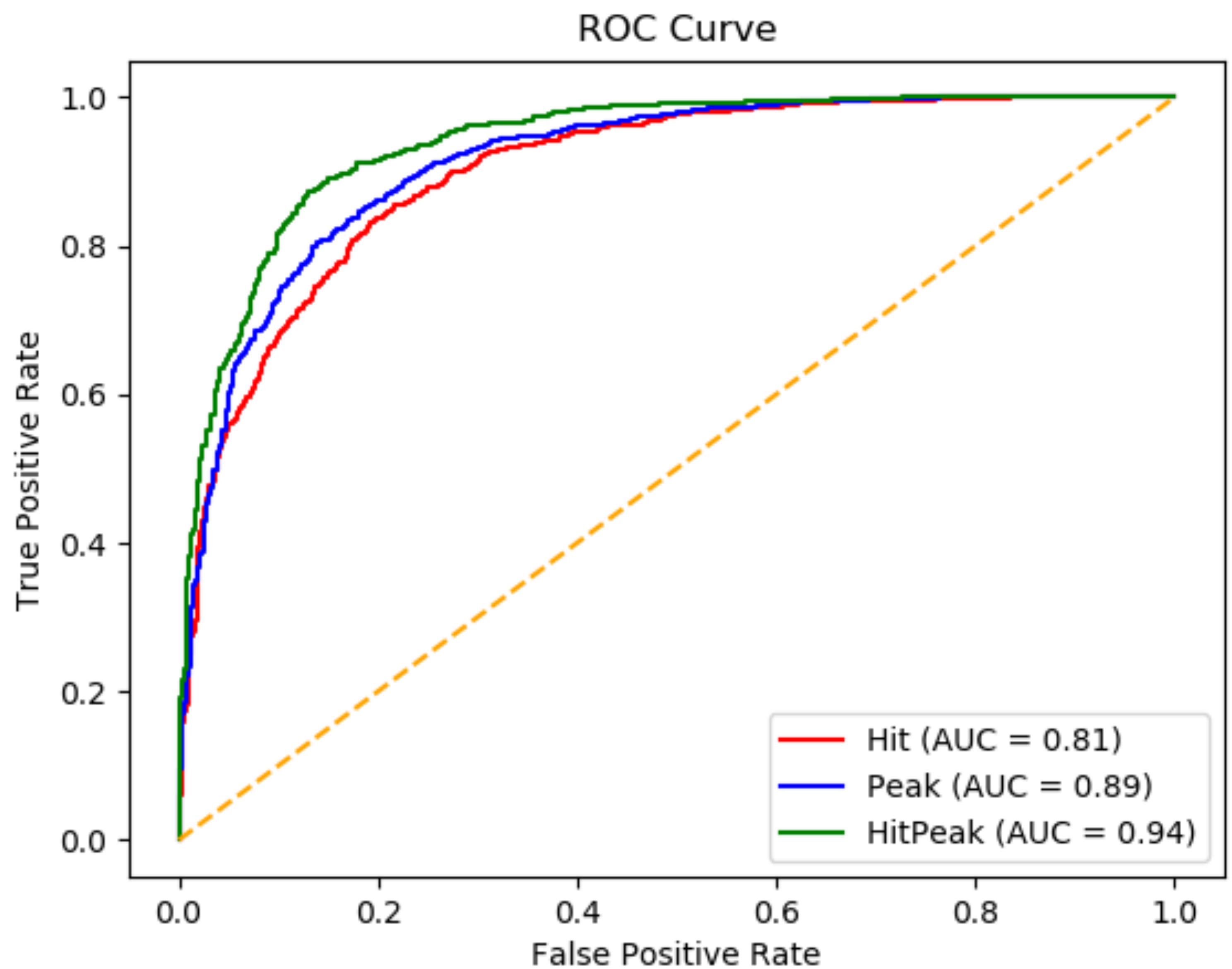

# Conclusions and Outlook

- We demonstrate the possibility of using ML for the Dark Matter Searches
- It shows the promising reach for disentangling among collider Dark Matter searches as well as for the direct detection experiments
- These works set the benchmark for the unsupervised anomaly detection methods

# Detector output can be viewed as images

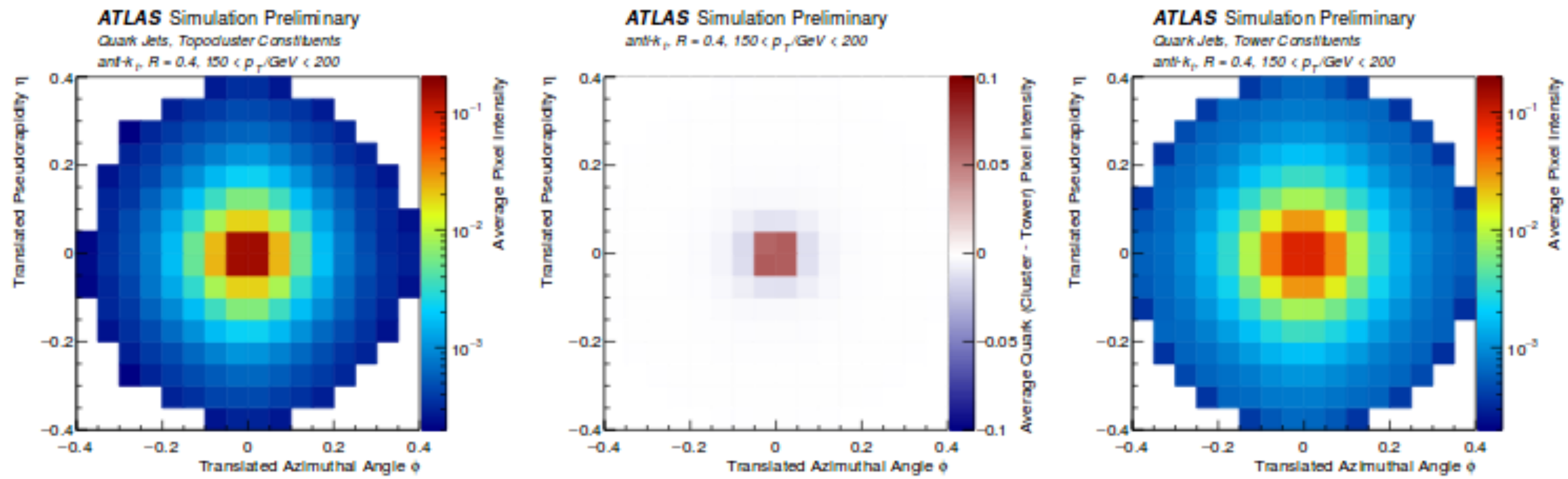


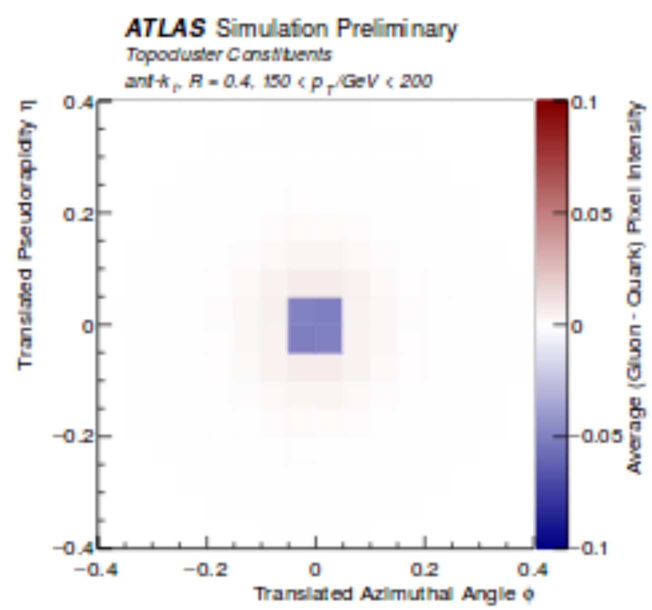


The ATLAS Collaboration. Quark versus Gluon Jet Tagging using Jet Images with the ATLAS Detector. Report No. ATL-PHYS-PUB-2017-017, https://cds.cern.ch/record/2275641 (CERN, 2017)
CMS Collaboration. New Developments for Jet Substructure Reconstruction in CMS. Report No. CMS-DP-2017-027, https://cds.cern.ch/record/2275226(CERN, 2017)

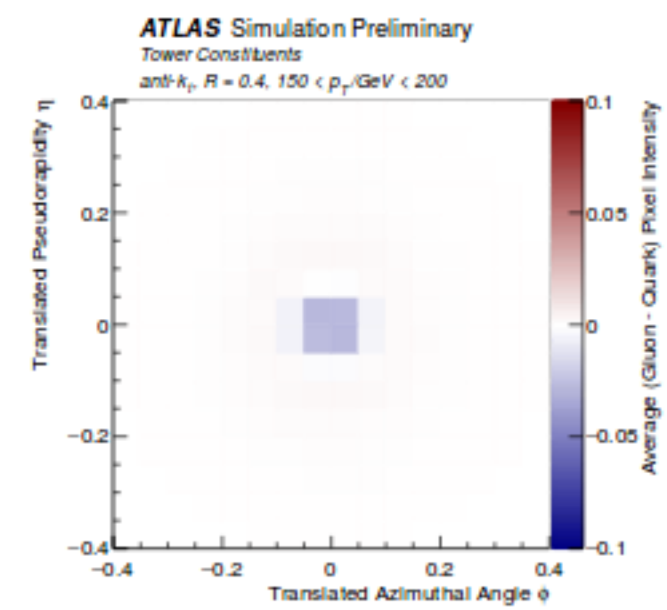


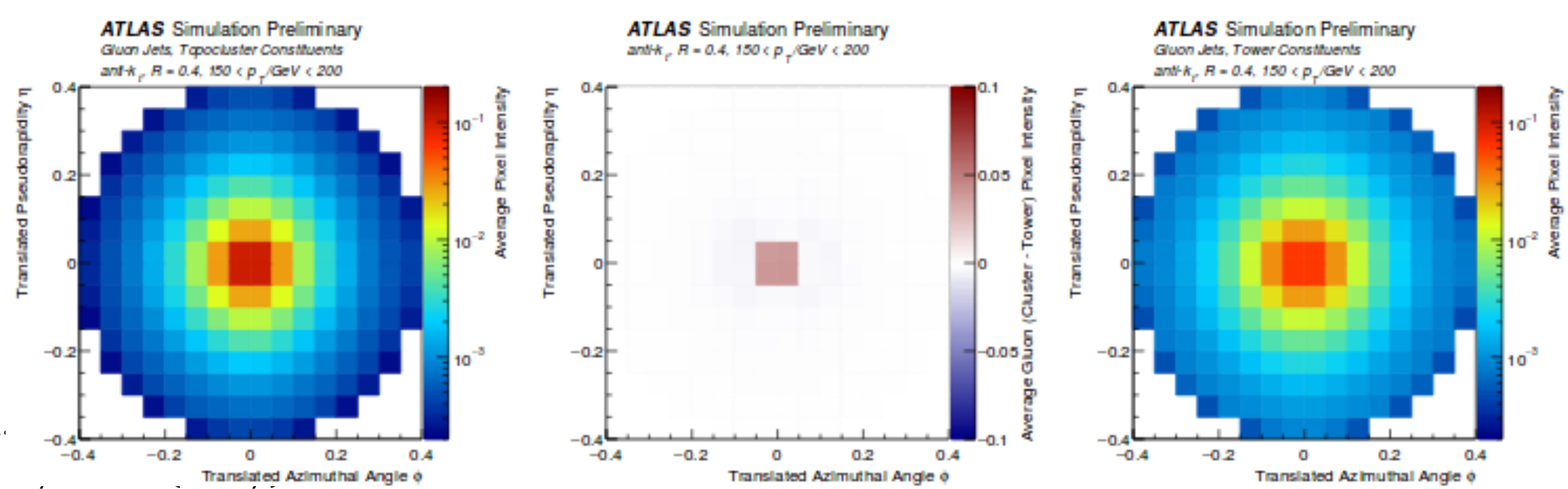


Neutrino Physics:

See e.g. Adamson, P. et al. in NOvA. Phys. Rev. D 96,

# PAX (Processor for Analysing Xenon)

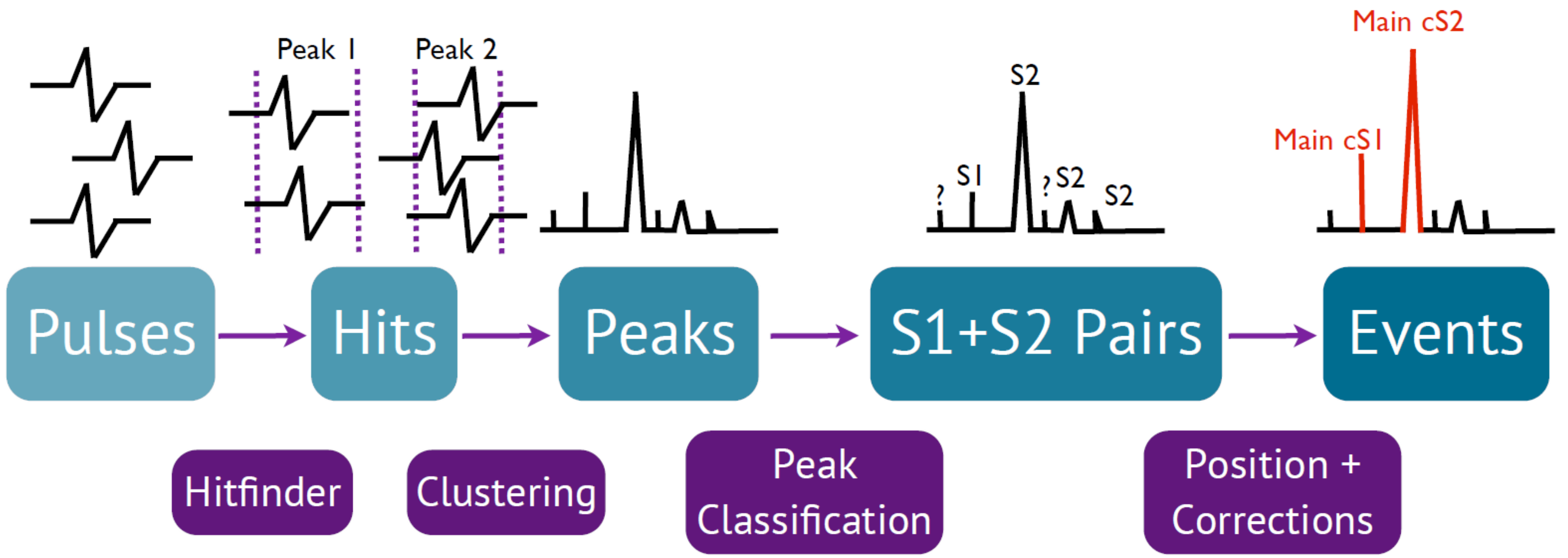


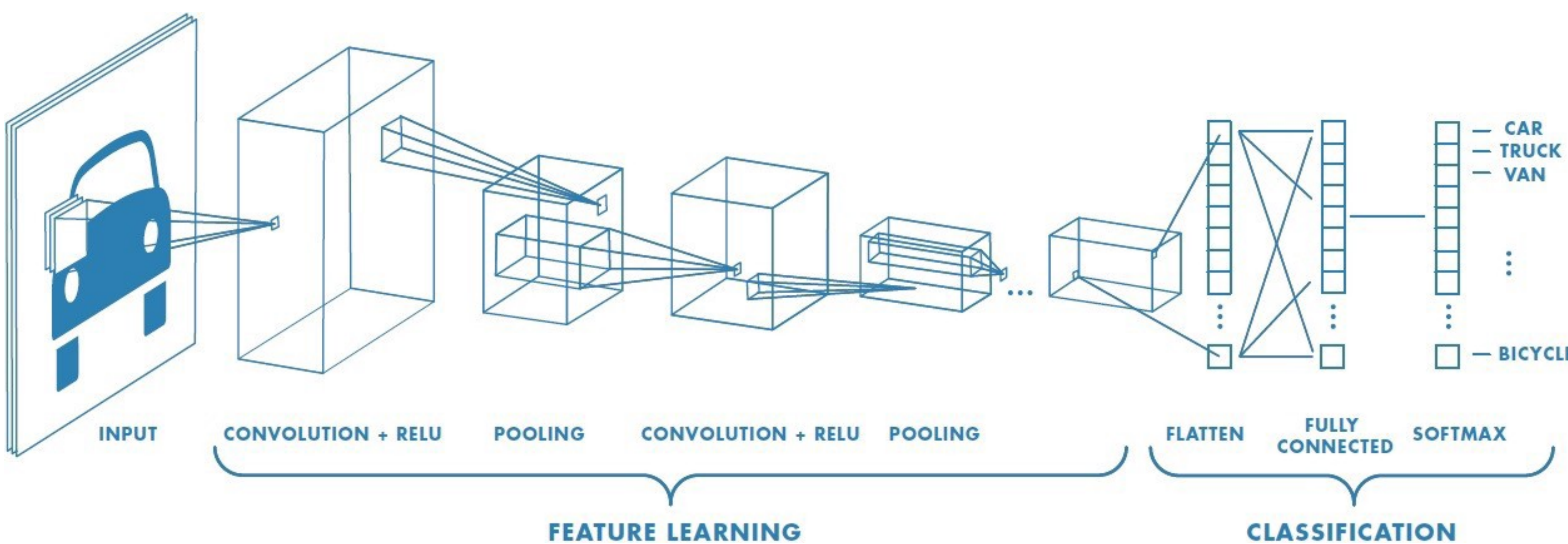

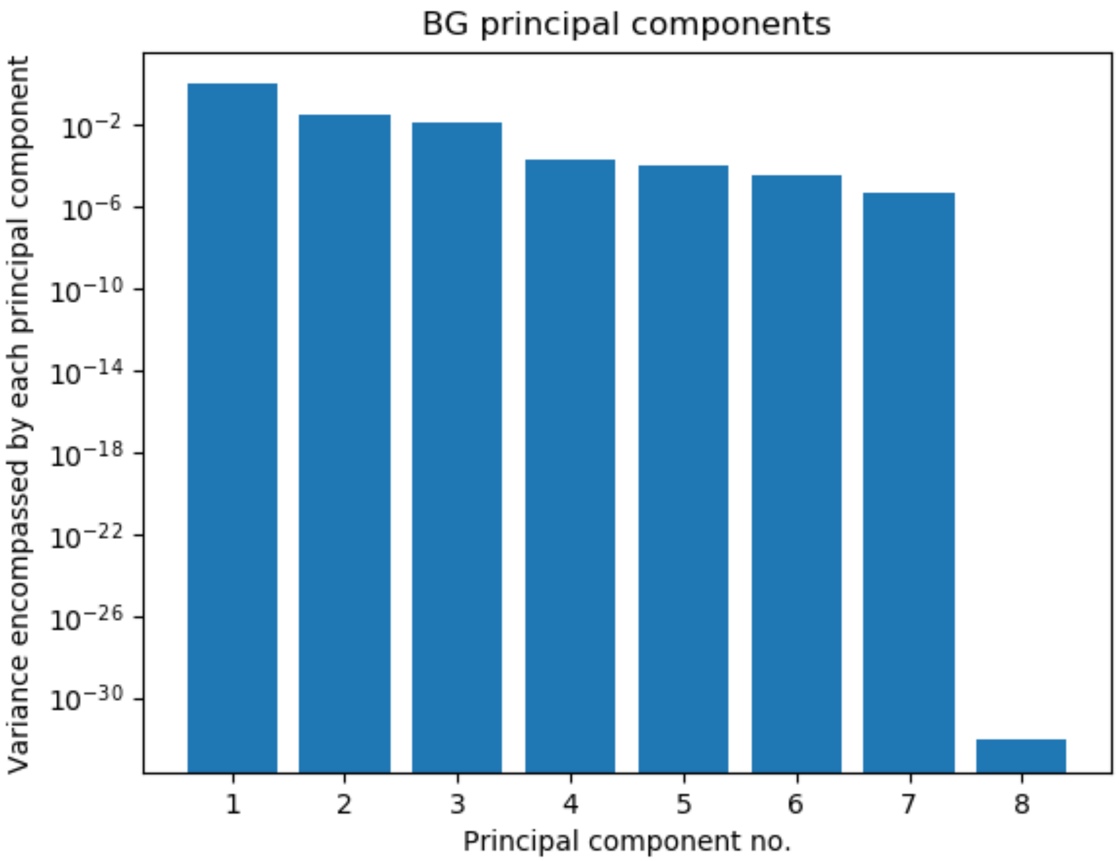


| Background PCA correlations | | | | | | | | |
|---|---|---|---|---|---|---|---|---|
| | $p_T^{j1}$ | $p_T^{j2}$ | $\eta_{j_1}$ | $\eta_{j_2}$ | $\Delta\phi_{j_1 j_2}$ | MET | $\Delta\phi^{j1}_{\mathrm{MET}}$ | $\Delta\phi^{j2}_{\mathrm{MET}}$ |
| PC-1 | 0.67 | 0.41 | -0.01 | -0.01 | -0.01 | 0.62 | 0.00 | -0.00 |
| PC-2 | 0.00 | 0.00 | 0.01 | 0.00 | 0.45 | -0.00 | -0.77 | -0.45 |
| PC-3 | -0.00 | -0.00 | 0.09 | 0.10 | -0.70 | -0.00 | 0.00 | -0.70 |
| PC-4 | -0.01 | 0.00 | -0.70 | -0.70 | -0.09 | -0.01 | -0.01 | -0.10 |
| PC-5 | -0.12 | 0.89 | -0.01 | 0.02 | -0.00 | -0.45 | 0.00 | 0.00 |
| PC-6 | -0.01 | 0.01 | 0.71 | -0.71 | -0.01 | -0.01 | 0.01 | -0.00 |
| PC-7 | 0.73 | -0.23 | 0.00 | 0.00 | 0.00 | -0.65 | 0.00 | 0.00 |
| PC-8 | 0.00 | 0.00 | -0.00 | -0.00 | 0.54 | -0.00 | 0.64 | -0.54 |

| SUSY3, $M_{\tilde{\chi}_1^0} = 300$ GeV PCA correlations | | | | | | | | |
|---|---|---|---|---|---|---|---|---|
| | $p_T^{j1}$ | $p_T^{j2}$ | $\eta_{j_1}$ | $\eta_{j_2}$ | $\Delta\phi_{j_1 j_2}$ | MET | $\Delta\phi^{j1}_{\mathrm{MET}}$ | $\Delta\phi^{j2}_{\mathrm{MET}}$ |
| PC-1 | 0.67 | 0.32 | 0.00 | 0.01 | 0.00 | 0.67 | -0.00 | -0.00 |
| PC-2 | -0.00 | -0.01 | 0.01 | -0.01 | 0.32 | -0.00 | -0.76 | -0.57 |
| PC-3 | 0.00 | -0.00 | -0.07 | -0.06 | -0.80 | 0.00 | 0.11 | -0.58 |
| PC-4 | -0.01 | 0.02 | 0.70 | 0.70 | -0.07 | -0.01 | 0.01 | -0.05 |
| PC-5 | -0.22 | 0.95 | -0.00 | -0.02 | 0.00 | -0.23 | -0.01 | -0.00 |
| PC-6 | -0.00 | 0.01 | -0.71 | 0.71 | 0.01 | -0.00 | -0.01 | -0.00 |
| PC-7 | 0.71 | -0.01 | -0.00 | 0.00 | -0.00 | -0.71 | 0.00 | 0.00 |
| PC-8 | 0.00 | 0.00 | 0.00 | -0.00 | 0.50 | 0.00 | 0.64 | -0.58 |

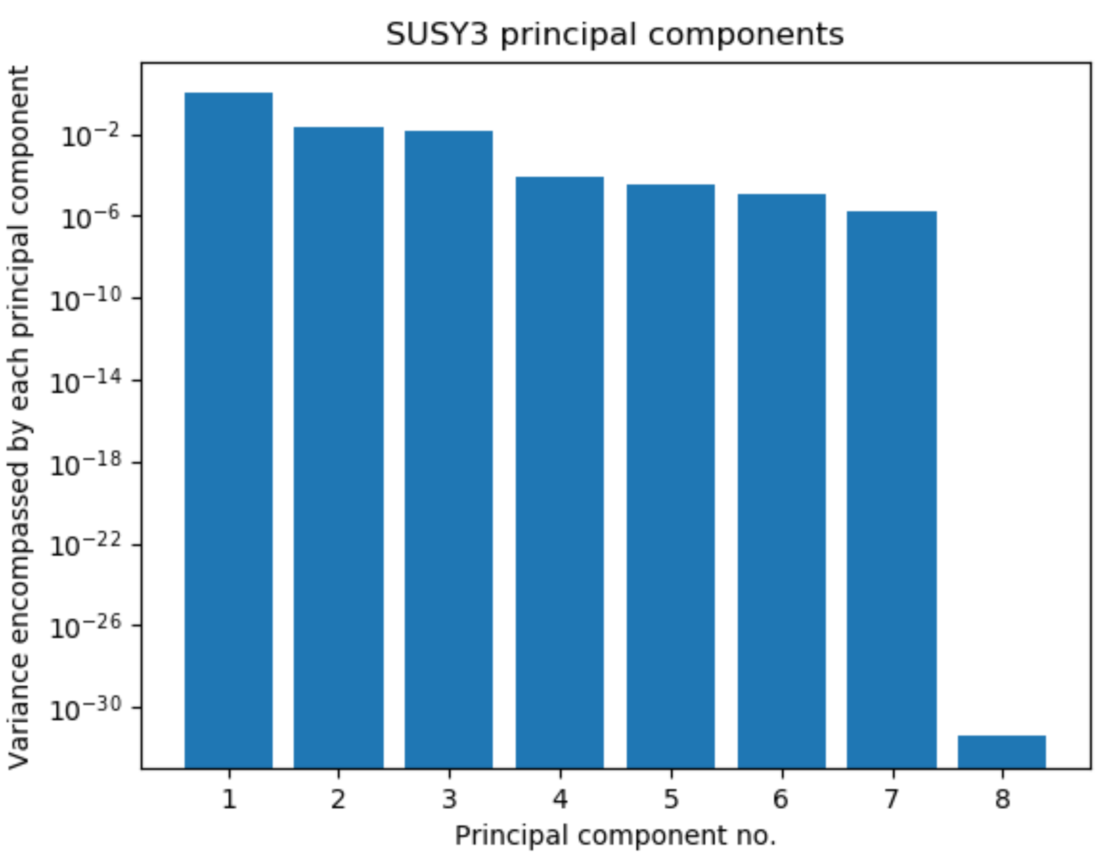

# Neural Network (NN): Basic Structure

**Training sample, validation sample, test sample**

- **Input layer nodes: set of observables(kinematical features)/images**
- **Number of hidden layers (shallow or deep NN)**
- **Output layer: predictions**

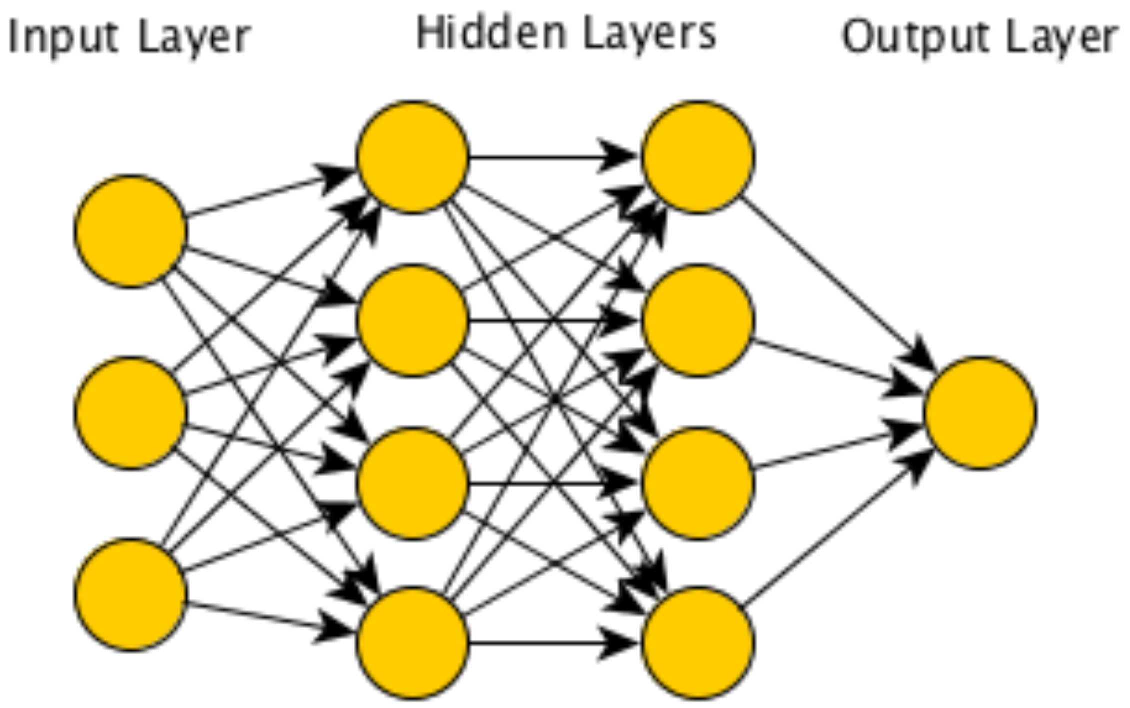


**Train the network using training sample and make predictions for the test set**